DNA Repair 78 (2019) 45–59

Contents lists available at ScienceDirect

DNA Repair

journal homepage: www.elsevier.com/locate/dnarepair

The three Endonuclease III variants of *Deinococcus radiodurans* possess distinct and complementary DNA repair activities

Aili Sarre[a], Meike Stelter[b], Filipe Rollo[c], Salvatore De Bonis[b], Anna Seck[b,e], Cécilia Hognon[d], Jean-Luc Ravanat[e], Antonio Monari[d], François Dehez[d], Elin Moe[a,c,**], Joanna Timmins[b,*]

[a] The Norwegian Structural Biology Centre (NorStruct), Department of Chemistry, UiT the Arctic University of Norway, N-9037 Tromsø, Norway
[b] Univ. Grenoble Alpes, CNRS, CEA, IBS, F-38000 Grenoble, France
[c] Instituto de Tecnologia Quimica e Biologica (ITQB), Universidade Nova de Lisboa, Av da Republica (EAN), 2780-157 Oeiras, Portugal
[d] LPCT, UMR 7019, Université de Lorraine, CNRS, Vandoeuvre-les-Nancy, France
[e] Univ. Grenoble Alpes, CEA, CNRS, INAC, SyMMES UMR 5819, Grenoble, France

ARTICLE INFO

Keywords:
Base excision repair
DNA glycosylase
Endonuclease III
Oxidative DNA damage
Deinococcus radiodurans
Radiation resistance
Catalytic activity

ABSTRACT

Endonuclease III (EndoIII) is a bifunctional DNA glycosylase that removes oxidized pyrimidines from DNA. The genome of *Deinococcus radiodurans* encodes for an unusually high number of DNA glycosylases, including three EndoIII enzymes (drEndoIII1-3). Here, we compare the properties of these enzymes to those of their well-studied homologues from *E. coli* and human. Our biochemical and mutational data, reinforced by MD simulations of EndoIII-DNA complexes, reveal that drEndoIII2 exhibits a broad substrate specificity and a catalytic efficiency surpassing that of its counterparts. In contrast, drEndoIII1 has much weaker and uncoupled DNA glycosylase and AP-lyase activities, a characteristic feature of eukaryotic DNA glycosylases, and was found to present a relatively robust activity on single-stranded DNA substrates. To our knowledge, this is the first report of such an activity for an EndoIII. In the case of drEndoIII3, no catalytic activity could be detected, but its ability to specifically recognize lesion-containing DNA using a largely rearranged substrate binding pocket suggests that it may play an alternative role in genome maintenance. Overall, these findings reveal that *D. radiodurans* possesses a unique set of DNA repair enzymes, including three non-redundant EndoIII variants with distinct properties and complementary activities, which together contribute to genome maintenance in this bacterium.

1. Introduction

DNA damage is a common occurrence that compromises the functional integrity of DNA. It is estimated that more than 10,000 bases are damaged daily in every human cell [1]. The causative agents of these damages are mainly free radicals (superoxide, hydroxyl radicals and hydrogen peroxide), which are normally produced as natural by-products of food metabolism. If damaged DNA is left unrepaired, it can generate mutations, replication errors, persistent DNA damage and genomic instability, which are ultimately associated with diseases, like cancer and premature aging.

The C5-C6 double bond of pyrimidines is vulnerable to attack by reactive oxygen species (ROS). The most ubiquitous lesions are 5-hydroxycytosine (5OHC) and 5-hydroxyuracil (5OHU) formed by oxidation of cytosine, and thymine glycol (Tg) formed by either oxidation of thymine or by oxidation and deamination of 5-methylcytosine [2,3]. Under anoxic conditions, dihydrothymine (DHT) and dihydrouracil (DHU) result from ionizing radiation damage to, respectively, thymine and cytosine [4,5]. DHU, 5OHU, and 5OHC can pair with adenine or cytosine during DNA synthesis and are therefore potentially mutagenic [6,7]. Of these lesions, Tg is the only one which is cytotoxic rather than mutagenic, having been shown to block DNA polymerases [8–10]. The reason is believed to be the relatively bulky perturbation it causes to the DNA structure.

Oxidized nucleobases are recognized and repaired by bifunctional DNA glycosylases belonging to the Base Excision Repair (BER) pathway. In humans, these lesions are excised by the hNeil1, hNeil2, hNeil3, hOgg1 and hNTH, while in *E. coli* the corresponding enzymes are Fpg, EndoVIII (Nei) and Endonuclease III (EndoIII). EndoIII enzymes have broad substrate specificity and remove a range of oxidized bases from

* Corresponding author at: Univ. Grenoble Alpes, CNRS, CEA, IBS, F-38000 Grenoble, France.
** Corresponding author at: The Norwegian Structural Biology Centre (NorStruct), Department of Chemistry, UiT the Arctic University of Norway, N-9037 Tromsø, Norway.
E-mail addresses: elin.moe@uit.no (E. Moe), joanna.timmins@ibs.fr (J. Timmins).

https://doi.org/10.1016/j.dnarep.2019.03.014
Received 20 December 2018; Received in revised form 26 March 2019; Accepted 27 March 2019
Available online 28 March 2019

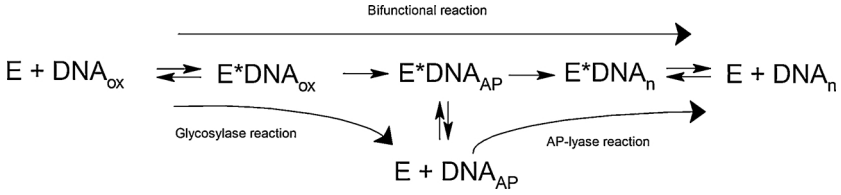

Fig. 1. Schematic representation of the bifunctional reaction mechanism catalyzed by EndoIII enzymes. In the case of coupled bifunctional activities, the enzyme and the substrate ($E + DNA_{ox}$) generate an enzyme-substrate complex (E^*DNA_{ox}), which leads to the removal of the oxidized base and the formation of a covalent enzyme-abasic site complex (E^*DNA_{AP}). In turn, this complex is further processed by the AP-lyase activity to an enzyme-nicked DNA complex (E^*_{DNAn}) and finally, the fully processed DNA product is released from the enzyme ($E + DNA_n$). In case the two reaction steps are uncoupled, the enzyme dissociates from the abasic site DNA ($E + DNA_{AP}$) after the glycosylase reaction. The enzyme can then engage in either one of the two sub-pathways: (i) a new round of DNA glycosylase activity on DNA_{ox} or (ii) AP-lyase activity on DNA_{AP}. The relative engagement into one or the other pathway depends on the concentrations of the various species (E, DNA_{ox}, DNA_{AP} and DNA_n) in the reaction.

DNA, but have Tg and 5OHC as their main substrates [11]. They belong to the Helix-hairpin-Helix (HhH) family of DNA glycosylases, which also includes the bacterial 3-methyladenine DNA glycosylase (AlkA), A/G mismatch DNA glycosylase (MutY) and human 8-oxoguanine DNA glycosylase (Ogg1). The crystal structures of EndoIIIs from *E. coli* (ecEndoIII) [12], *D. radiodurans* (drEndoIII1 and drEndoIII3) [13] and *B. stearothermophilus* (bstEndoIII) [14] have been determined in either their apo- or DNA-bound form. They consist of a two domain helical bundle structure, separated by a positively charged DNA binding cleft. The cleft contains the highly conserved DNA-binding HhH motif, three less conserved DNA-interacting loops (FCL, DIL1 and DIL2), and the active site [12–14]. A superimposition of all HhH DNA glycosylases shows that the structure of EndoIII is very similar to the core structure of other members of this family, however only EndoIII and MutY enzymes possess a [4Fe-4S] cluster. The role of this cluster is still unclear. It was initially suggested to play only a structural or regulatory role [15]. Lately it has been shown to be redox activated upon binding to both DNA [16] and other positively charged entities [17].

The bifunctional activity of EndoIII enzymes, illustrated in Fig. 1, includes removal of the damaged base through scission of the glycosidic bond between the base and the ribose (DNA glycosylase activity) followed by cleavage of the DNA backbone (AP-lyase activity) on the 3' side of the abasic site, leaving a 3'-unsaturated aldehyde and a 5'-phosphate group at the ends of the DNA [18,19]. Thereafter the unsaturated aldehyde is processed by an AP-endonuclease in bacteria in order to prepare the ends for incorporation of the correct base by a DNA polymerase followed by ligation by a DNA ligase. While monofunctional DNA glycosylases depend on a highly conserved aspartate for hydrolysis of the N-glycosidic bond, an additional highly conserved lysine is important for activity of the EndoIII enzymes [12,20]. This lysine is proposed to be the main catalytic residue responsible for cleavage of the N-glycosidic bond by nucleophilic attack on the anomeric carbon, thereby forming a transient enzyme-DNA Schiff base complex that has been trapped covalently in numerous studies [14,21,22]. Formation of the complex facilitates proton abstraction at C2' of the ribose, leading to subsequent nicking of the DNA by beta-elimination of the C3' phosphate bond. The proton abstraction is believed to be important for this step [23], and Fromme et al. [14] have suggested that a second conserved aspartate (D45 in bstEndoIII) is responsible for this activity.

Most studied EndoIII enzymes display concerted bifunctional activity; however, the human EndoIII (hNTH) has in several studies displayed a higher DNA glycosylase activity than AP-lyase activity [24–26]. Such uncoupling of activities is also observed in two other eukaryotic DNA glycosylases that repair ROS induced damage, hOgg1 [27,28] and hNeil3 [29]. In these bifunctional DNA glycosylases, the individual reaction steps take place in a non-concerted manner, thereby creating two separate sub-pathways, as illustrated in the kinetic scheme in Fig. 1. Marenstein et al. [25] explain the uncoupling as a consequence of hNTH's poor affinity towards the intermediate, the abasic or Ap site, leading to dissociation of the enzyme-Ap-DNA complex before the beta-elimination.

The genome of the extreme radiation- and desiccation-resistant bacterium, *D. radiodurans,* encodes an unusually high number of DNA glycosylases including three EndoIII-like enzyme variants: DR2438 (drEndoIII1), DR0289 (drEndoIII2) and DR0982 (drEndoIII3) [30,31]. Interestingly, *D. radiodurans* does not possess a homologue of *E. coli* Nei/EndoVIII DNA glycosylase. Previously, we had determined the crystal structures of drEndoIII1 and drEndoIII3, and generated a homology model of drEndoIII2 [13], which we have further validated using molecular dynamics (MD) simulations in the present study (Fig. S1). Our structure-function analysis of these enzymes revealed that the structures of the three drEndoIIIs are very similar to those of ecEndoIII and bstEndoIII [12,14], but only drEndoIII2, and to a lesser extent drEndoIII1, possess bifunctional activity towards Tg and AP-lyase activity on Ap-DNA. DrEndoIII3, despite its preserved fold and conserved catalytic residues, displayed no activity on such substrates. We hypothesized at the time that the differences in activity may be attributed to altered electrostatic surface potentials, modified substrate binding pockets and amino acid substitutions in the DNA binding loops [13].

Here, we present an in-depth analysis of the activity and substrate specificities of the three drEndoIII enzymes and have compared them to those of their well-studied homologues from *E. coli* (ecEndoIII) and human (hNTH). We demonstrate that drEndoIII2 is a highly efficient EndoIII enzyme with catalytic properties that surpass those of ecEndoIII and hNTH, and with broad substrate specificity. DrEndoIII1, in contrast, displays only weak activity on classical EndoIII substrates, with a clear uncoupling of its DNA glycosylase and AP-lyase activities, a feature of eukaryotic DNA glycosylases. Interestingly it was also found to process single stranded DNA (ssDNA) substrates. The third variant, drEndoIII3 shows no detectable enzymatic activity on oxidized bases, but, surprisingly, possesses the highest affinity for damaged DNA of the three enzymes, indicating that it may play an alternative role in the DNA repair process.

2. Materials and methods

2.1. Expression and purification of EndoIII and Fpg enzymes

Wild-type and mutant genes encoding *Deinococcus radiodurans* EndoIII enzymes were cloned, expressed and purified as described previously [13,32]. In the present study, drEndoIII3 corresponds to the N-terminally truncated form of the (mis)annotated drEndoIII3 (DR0982) described previously [13,32], and residue numbering assumes that V76 in DR0982 is an alternative start codon and is thus numbered 1. The conserved catalytic residues discussed in this study (K156, D174 and R64) thus correspond respectively to K231, D249 and R139 in the original annotated protein sequence. Mutants were constructed using Stratagene QuickChange Mutagenesis Kit on the pDest14 plasmid containing wild type genes. The mutants were expressed and purified as described for the wild-type enzymes [13,32]. *E. coli* EndoIII was also cloned into the pDest14 expression vector and expressed and purified following the same protocol as used for drEndoIII2 [13,32]. A synthetic gene optimized for *E. coli* expression (Shinegene) and coding for human NTH was cloned into pET21a for expression as an N-terminally His-tagged protein in *E. coli* BL21 cells. hNTH expression was

induced with 1 mM IPTG at 20 °C for 16 h. Cell pellets were lysed in buffer A composed of 50 mM Tris pH 8.0, 500 mM NaCl, 0.5 mM EDTA, 0.02% Triton X-100 and 5% glycerol, supplemented with protease inhibitor tablets (Roche), DNase I (Roche) and lysozyme (Roche). The cleared supernatant was purified on a HisTrap FF column (GE Healthcare) and eluted with buffer A supplemented with 250 mM imidazole. hNTH was then dialysed against 20 mM Tris pH 8.0, 300 mM NaCl, 0.5 mM EDTA, 0.01% Triton X-100, 10% glycerol and 1 mM β-mercaptoethanol (βME), and further purified on a HiTrap S column (GE Healthcare). hNTH was eluted with a NaCl gradient, concentrated and separated on a Superdex 200 (GE Healthcare) size-exclusion column equilibrated in 20 mM Tris pH 8.0, 300 mM NaCl, 0.5 mM EDTA, 0.005% Triton X-100, 1 mM βME, 10% glycerol. The gene encoding *D. radiodurans* Fpg/MutM (DR0493) was amplified by PCR and sub-cloned into pET21a for expression in BL21 (DE3) Star cells with a cleavable C-terminal His-tag. DrFpg expression was induced with 1 mM IPTG at 37 °C for 4 h. Cell pellets were lysed in buffer B composed of 50 mM Na-Phosphate pH 7.0 and 300 mM NaCl, supplemented with protease inhibitor tablets (Roche), DNase I (Roche) and lysozyme (Roche). The cleared supernatant was purified on a HisTrap FF column (GE Healthcare) and eluted with buffer B supplemented with 250 mM imidazole. DrFpg was then incubated with TEV protease to remove the His-tag and dialysed against 50 mM Na-Phosphate pH 7.0 and 100 mM NaCl overnight. The cleaved protein was further purified on a second Ni-NTA column and subsequently loaded onto a 1 ml MonoS column (GE Healthcare). Finally, DrFpg was eluted with a NaCl gradient, concentrated and separated on a Superdex 75 (GE Healthcare) size-exclusion column equilibrated in 50 mM Tris pH 7.0 and 150 mM NaCl). All enzymes were concentrated to 5–10 mg/ml and stored at −80 °C for the activity measurements.

2.2. Molecular beacon

The sequences of the molecular beacon DNA used in this study are given in Table S1. The molecular beacon assay was performed at 37 °C with 1 nM to 1.5 μM beacon DNA and 10 nM drEndoIII2 or 100 nM drEndoIII1, hNTH and ecEndoIII in a buffer composed of 20 mM Tris pH 7.5, 150 mM NaCl, 2 mM βME, 0.01% Triton X-100, 0.5 mM EDTA and 0.1 mg/ml BSA. Reactions were performed in black NBS (no binding surface) 384-well plates (Corning) in reaction volumes of 80 μl and were started by the addition of enzyme. Upon cleavage of the phosphate backbone, fluorescence emission at 520 nm (excitation at 485 nm) was recorded on a Clariostar (BMG Labtech) microplate reader in kinetics mode (measurements were made every 15 s over a period of 75 min). Fluorescence values in response units were converted to DNA concentrations using a standard curve obtained by measuring the fluorescence emission of 10, 50, 150, 500, 750, 1000 and 1500 nM beacon DNA heated to 100 °C for 5 min in the presence of 5 μM target DNA. All measurements were performed at least in triplicate. For each beacon concentration, initial velocities were determined by fitting a linear regression curve to the linear region of the kinetic curves. The average rates from three independent experiments were plotted against the beacon concentration and the curves were fitted to a classical Michaelis-Menten model using GraphPad Prism6 to determine values for the Michaelis constant, K_m, and the maximum velocity, V_{max}. The catalytic kinetic constant (K_{cat}) was calculated by dividing V_{max} by the enzyme concentration.

2.3. Activity assays

Gel-based activity measurements were performed using 5'-FAM labeled 35 nt dsDNA oligonucleotides (oligos) with a modified nucleobase in position 14 (Table S1). Oligos containing oxidized bases (Tg, 5OHC, 5OHU, DHT, DHU, U) were synthesized by Midland Certified Reagent Co. and complementary strands were purchased from MWG Eurofins. All oligos were dissolved in 10 mM Tris pH 8.0 and 45 mM NaCl and double-stranded substrates were obtained by annealing the FAM-labeled lesion-containing strands with each of the four possible complementary oligos containing either adenine, cytosine, guanine or thymine opposite the damage with a slight surplus of the non-labeled reverse strand to a final concentration of 50 μM. Abasic site (Ap) containing DNA substrate was prepared by treating the uracil containing 5'-FAM tagged 35-nt oligo with *D. radiodurans* Uracil DNA-glycosylase (drUNG) [33]. The complementary strand had a guanine in the position opposite the uracil. The enzyme was diluted to 1 μM in 50 mM Tris pH 7.5 and 150 mM NaCl. In a 20 μl reaction volume, 1 μM 35 nt-dU-eG was mixed with 0.1 μM drUNG and the reaction was incubated for 30 min at 37 °C. After incubation, the reaction was stopped by heat-inactivation (95 °C for 2 min) of the enzyme.

Initial substrate specificity assays were performed in 15 μl reactions containing 1 μM DNA and either 1 or 10 μM enzyme in 50 mM Tris pH 7.5 and 150 mM NaCl. Reactions were incubated at 37 °C for either 30 or 60 min. Control samples were incubated without enzyme. In end point assays the native and/or mutant enzyme-DNA mixes were incubated at 37 °C in a master mix with 50 mM Tris pH 7.5, 150 mM NaCl and 0.1 mg/ml BSA, for 30 or 60 min, with 75 nM of DNA (dsDNA or ssDNA) and 75 nM enzyme. In the time course assays, enzyme-DNA mixes were incubated at 37 °C in a master mix with 50 mM Tris pH7.5, 150 mM NaCl and 0.1 mg/ml BSA (supplemented with 2 mM βME and 0.01% Triton X-100 in the case of hNTH). The DNA substrate concentration was kept constant at 75 nM and enzyme concentrations were varied between 3 nM to 750 nM for each assay. All reactions were stopped by adding 2X denaturing buffer (2X TBE, 8 M urea, 0.025% bromophenol blue, 0.025% SDS buffer), heating at 95 °C for 2 min, followed by NaOH (0.1 M) treatment of half of the reactions in order to analyze the DNA glycosylase activity. The other half was used to analyze AP-lyase activity. Samples were then loaded on 20% 8 M Urea PAGE gels that had been prerun for 30 min at 5 W per gel. Gels were run for 30 min at 5 W per gel, and DNA bands were visualized using a ChemiDoc MP imager (Biorad) and analyzed using ImageLab (Biorad). Lanes and bands were fitted manually and quantified with the lane profile tool. To determine initial velocities, the early time points were fitted to a linear regression and the derived slopes correspond to the initial rates. Significance of uncoupling of DNA glycosylase and AP-lyase activities was determined by a paired *t*-test, significant processing was determined by one-sample *t*-test and significant differences among samples were determined by 1-way ANOVA tests.

2.4. HPLC-MS-MS analysis of 8-oxo-G processing

8-oxo-guanine (8-oxo-G) lesions were introduced into pUC19 plasmid using the photosensitization method relying on riboflavin [34]. 400 μg pUC19 was oxygenized continuously for 15 min before addition of 177 μM riboflavin. The DNA was then exposed to a halogen lamp for 2 min at a distance of 20 cm. After irradiation, the plasmid was precipitated with 0.4 M NaCl and ice-cold 100% ethanol and resuspended in H_2O. 240 ng of 8-oxo-G containing plasmid DNA was incubated with 100 nM or 1 μM enzyme (drEndoIIIs, ecEndoIII or drFpg) in 50 mM Tris pH 7.5, 150 mM NaCl and 0.1 mg/ml BSA at 37 °C for 30 min. Part of the reactions (80 ng plasmid) were separated on 1% TBE agarose gel and stained with Gel Red. The rest was used for HPLC-MS-MS analysis of 8-oxo-G subsequently to DNA hydrolysis as described previously [35].

2.5. DNA binding assays

Equilibrium fluorescence anisotropy DNA binding assays were performed on a Clariostar (BMG Labtech) microplate reader, fitted with polarization filters to measure fluorescence anisotropy. The binding assays were conducted in 384-well plates at room temperature in 40μl reaction volumes in a buffer composed of 10 mM Tris pH 7.5, 150 mM NaCl and 0.05% Tween. A fixed concentration (10 nM) of a 5'-FAM

labeled 16mer dsDNA containing a tetrahydrofuran (THF) Ap site in position 9 (Table S1) was mixed with increasing concentrations of each enzyme. After subtracting the polarization values obtained for DNA alone, the mean data from three independent experiments were fitted to a standard binding equation ($Y = Bmax*X^h/(Kd^h + X^h)$) assuming a single binding site with Hill slope (h) using GraphPad Prism6, where Y is the difference between the anisotropy of completely bound and completely free oligo, X is the enzyme concentration and Kd is the equilibrium dissociation constant [36]. The fits were very good, with R^2 values all above 0.98.

DNA bandshift assays were performed as described previously [13]. For the opposite base preference and substrate affinity experiment a 5'-FAM labeled 20 mer DNA duplexes containing either an intact base, a THF or a natural Ap site opposite A, G, C or T were used (Table S1). The natural Ap site was prepared as follows: 6 pmol 20 mer-dU dsDNA was mixed with 0.2 pmol cod UNG in 50 mM Tris pH 7.5 and 150 mM NaCl, and the reaction was incubated for 90 min at 37 °C. The reaction was stopped by heat-inactivation (95 °C for 2 min) of the enzyme. To evaluate the binding of drEndoIII1 to the product of the bifunctional activity (the nicked AP-DNA), 1 μM 5'-FAM labeled 35 mer DNA substrate containing Tg opposite G (Table S1) was incubated with 0.5 μM drEndoIII2 in a 20 μl reaction volume at 37 °C for 60 min. 0.1 μM nicked AP-DNA was then incubated at 4 °C for 30 min in a 10 μl reaction containing 0, 0.125, 0.5, 2.0 and 8.0 μM drEndoIII1 prior to gel electrophoresis as described previously [13].

2.6. MD simulations

The initial structures of drEndoIII1 and drEndoIII3 were those determined in our previous investigation (pdb 4UNF and 4UOB pdb, respectively) [13]. For drEndoIII2, a homology model was built based on the crystal structure of ecEndoIII (pdb 2ABK) [13]. MD simulations were performed on the apo-drEndoIII structures to verify the stability of the models (Fig. S1). The starting models of drEndoIII-DNA complexes were prepared by overlaying drEndoIII structures on Domain B (helices αB to αG) of bstEndoIII bound to an 11mer THF-Ap-DNA with guanine as the estranged base (PDB 1P59). No reliable starting model for drEndoIII1 bound to DNA could be prepared due to a large number of steric clashes (Fig. S2), consequently, no MD simulations of DNA complexes using drEndoIII1 were performed. The DNA containing Tg model was prepared by replacing the THF Ap site in the DNA duplex with Tg extracted from the structure of hNeil in complex with Tg-DNA (pdb 3VK8). In these starting models (Fig. S2), the Tg moiety was positioned in the center of the substrate binding pocket while preventing steric clashes. Following a similar procedure, drEndoIII2- and drEndoIII3-DNA complexes with adenine as the estranged base were further constructed. All the molecular systems were explicitly hydrated in boxes of ~ 42,000 water molecules containing 22 sodium ions to ensure the overall electrical neutrality of the unit cells.

Water was represented by means of the TIP3P water model [37], whereas protein, DNA and ions were described using the amberf99 force field [38] including the bsc1 corrections for DNA [39]. The [4Fe-4S] clusters of drEndoIIIs were modeled using the set of parameters designed specifically by Carvalho and Swart for the AMBER force field [40,41]. Parameters for nucleotides containing Tg were extracted from the amberf99 force field, point charges were fitted against the quantum chemical electrostatic potential computed at the HF/6-31G level. Parameters for the Ap lesions were taken from our previous work [42,43]. All setups were generated using the tleap facility of Amber Tools [44,45]. Molecular rendering and analyses were done using VMD [46]. MD simulations were performed using the massively parallel code NAMD [47]. All trajectories were generated in the isobaric-isothermal ensemble, at 300 K under 1 atm using Langevin dynamics [48] (damping coefficient 1 ps^{-1}) and the Langevin piston method [49], respectively. Long-range electrostatic interactions were accounted for by means of the Particle Mesh Ewald (PME) algorithm [50]. The rattle algorithm was used to constrain lengths of covalent bonds involving hydrogen atoms to their equilibrium value [51]. The classical equations of motion were integrated through a multiple time-step algorithm with a time step of 2 and 4 fs for short- and long-range interactions, respectively [52]. Each molecular assay was thermalized during 15 ns, followed by 500 ns of data acquisition. For the 11 molecular systems studied here, the total aggregated simulation time amounts to ~5.5 μs.

3. Results

3.1. Substrate specificity

We have previously confirmed that two of the *D. radiodurans* EndoIII enzymes, drEndoIII1 and drEndoIII2, possess activity towards Tg [13]. To further investigate variations in the substrate specificities of the drEndoIII enzymes, we performed gel-based activity assays with a diverse set of fluorescently labeled DNA substrates containing one of the following oxidized pyrimidine bases: Tg, 5OHC, 5OHU, DHT, DHU or U, paired with each of the four normal bases. The screen was performed under single-turnover (STO) conditions (with a 10-fold excess of enzyme). Both the DNA glycosylase and the bifunctional activities of the EndoIIIs were assessed after 1 h. Under these STO conditions, however, the extent of DNA glycosylase and AP-lyase processing were indistinguishable and only the results of the bifunctional processing are presented in Table 1.

The results show that both drEndoIII1 and drEndoIII2 are bifunctional DNA glycosylases with broad and overlapping substrate specificities, while drEndoIII3 showed no activity towards any of the tested substrates. drEndoIII2 displayed stronger activity and broader specificity than drEndoIII1, completely processing all substrates, except for uracil, for which it had a clear preference for guanine as the paired base. DrEndoIII1 performed complete cutting of the three ring-saturated substrates (Tg, DHT, and DHU), but showed reduced activity towards 5OHU and very little activity against 5OHC. It displayed no detectable activity on uracil-containing substrates. Interestingly, for

Table 1
Substrate specificity screen of drEndoIII enzymes under STO conditions (1 μM DNA and 10 μM EndoIII) on DNA lesions: Tg, 5OHC, 5OHU, DHU, DHT and U base-paired with either G, A, C or T. The bifunctional activity was assessed by gel electrophoresis. -: no detected activity, +: < 25% excised, + +: between 25 and 50% excised, + + +: between 50 and 75% excised, + + + +: > 75% excised.

Lesion	Estranged base	drEndoIII1	drEndoIII2	drEndoIII3
Tg	G	+ + + +	+ + + +	–
	A	+ + + +	+ + + +	–
	C	+ + + +	+ + + +	–
	T	+ + + +	+ + + +	–
5OHC	G	+	+ + +	–
	A	+	+ + +	–
	C	+	+ + +	–
	T	+	+ + +	–
5OHU	G	+ + +	+ + + +	–
	A	+	+ + + +	–
	C	+ + +	+ + + +	–
	T	+ + +	+ + + +	–
DHU	G	+ + + +	+ + + +	–
	A	+ +	+ + + +	–
	C	+ + + +	+ + + +	–
	T	+ + + +	+ + + +	–
DHT	G	+ + + +	+ + + +	–
	A	+	+ +	–
	C	+ + + +	+ + + +	–
	T	+ + + +	+ + + +	–
dU	G	–	+ + +	–
	A	–	–	–
	C	–	–	–
	T	–	–	–

5OHU, DHT or DHU, drEndoIII1's activity was drastically reduced when paired with adenine.

8-Oxoguanine (8-oxo-G) is one of the most common DNA lesions resulting from reactive oxygen species and is known to be efficiently repaired by Fpg/MutM enzymes [53]. To investigate whether 8-oxo-G could possibly be a substrate of drEndoIII3, we incubated 8-oxo-G containing plasmid DNA with each of the three drEndoIII enzymes and *D. radiodurans* Fpg (drFpg). HPLC coupled to tandem mass spectrometry was used to determine the levels of 8-oxo-G in each of the samples. These data clearly demonstrated that none of the EndoIII enzymes processed 8-oxo-G in contrast to drFpg which recognized and released 8-oxo-G in a concentration-dependent manner (Fig. S3). Also, the analysis of the 8-oxo-G plasmid reactions by gel electrophoresis revealed that drEndoIII2 and to a lesser extent drEndoIII1, were able to nick the plasmid in a concentration-dependent manner (Fig. S3), indicating that additional lesions (other than 8-oxo-G) were introduced into the plasmid DNA during the photosensitization reaction, that could be processed by EndoIII enzymes. These lesions are most likely further oxidation products of 8-oxo-G, such as hydantoin derivative, which have previously been reported to be processed by EndoIIIs [54]. Here again, drEndoIII3 showed no activity on such lesions.

3.2. Catalytic efficiency towards common oxidized pyrimidines

The DNA glycosylase and AP-lyase activities of drEndoIII1 and drEndoIII2 on oxidized pyrimidines paired with either adenine or guanine were then compared to those of their well-studied homologues: ecEndoIII and human NTH (Fig. 2). These measurements confirm that drEndoIII2 possesses a very broad substrate specificity and is a highly active enzyme, with a bifunctional activity on all substrates tested that is equivalent to, or surpassing, that of ecEndoIII and hNTH. On all substrates tested, it exhibited the highest processing efficiency. It fully excised 5OHU, whereas hNTH only processed 55% of this substrate, and it fully processed DHT:A, while ecEndoIII only cleaved ~50% of this substrate. This similarity between drEndoIII2 and its homologues in terms of activity was also confirmed at the structural level when preparing drEndoIII2-DNA models for MD simulations using the bstEndoIII homologue bound to DNA. A reliable model could be prepared without any structural rearrangements (Fig. S2), indicating that drEndoIII2 is also structurally the most similar to previously studied EndoIII enzymes.

Although drEndoIII1 recognized the same substrates, it displayed considerably lower activities, typically 5–40% of drEndoIII2's activity under these conditions, with Tg paired with guanine being its preferred substrate. Also, while the two enzymatic activities of drEndoIII2, hNTH and ecEndoIII at a 1:1 enzyme:DNA ratio appear to be fully coupled (i.e. the DNA glycosylase and bifunctional activities are very similar), the monofunctional DNA glycosylase activity of drEndoIII1 appears to be higher than its bifunctional activity. This uncoupling effect is particularly clear on Tg-containing DNA substrates (Fig. 2A and B) and suggests that the AP-lyase activity of drEndoIII1 is less efficient than its glycosylase activity.

To further compare the kinetic parameters of the two active drEndoIII enzymes to that of their homologues, we performed a molecular beacon assay (Fig. S4). The molecular beacon contained either a Tg paired with adenine or a 5OHC paired with guanine (Table S1), and the assay measured bifunctional processing of these substrates at various substrate concentrations. The kinetic parameters derived from this data are presented in Table 2. With the 5OHC containing beacon, the data recorded for drEndoIII1 did not reach a plateau and as a result no reliable kinetic parameters could be extracted from this data, thereby confirming our earlier findings that 5OHC is a poor substrate for drEndoIII1 (Table 1 and Fig. 2). DrEndoIII2 proved to be the enzyme with the highest catalytic efficiency (K_{cat}/K_m) towards both substrates and exhibits the characteristics of a highly efficient bacterial EndoIII enzyme, while drEndoIII1 displayed the lowest efficiency of all four homologues, confirming our results from gel-based assays (Fig. 2). The catalytic efficiencies of drEndoIII2 towards 5OHC:G and Tg:A were determined to be respectively, two and three times that of ecEndoIII, and nine and six times higher than that of hNTH. The marked difference in catalytic efficiency that we observed between ecEndoIII and hNTH is in agreement with earlier studies [55–58] and has been proposed to result from slow release of the product in the case of hNTH [59]. The remarkable enzymatic efficiency of drEndoIII2 is primarily due to its higher turnover rates (K_{cat}) on both DNA substrates. DrEndoIII2 displays a relatively poor apparent affinity for the two lesions with K_m values, which are similar to that of ecEndoIII, but 5–10 times higher than for hNTH.

DrEndoIII1 stands out among the four enzymes as having the poorest catalytic efficiency on Tg, with values 200 times lower than that of drEndoIII2, and 30 times lower than hNTH. Its turnover rate is comparable to that of hNTH, being 80–100 times slower than the two bacterial homologues. The main reason for its poor activity is its exceptionally low apparent affinity for the Tg substrate. Its K_m value for Tg-DNA was determined to be 500 times higher than that of hNTH and 4 times higher than that of drEndoIII2 and ecEndoIII. Our equimolar gel-based activity assays (Fig. 2), however, indicated that the AP-lyase activity of drEndoIII1 is weaker than its glycosylase activity. Since the molecular beacon assay only allows us to determine the overall kinetic parameters of the complete bifunctional reaction, the kinetic constants for the glycosylase reaction on Tg substrate may be significantly better for drEndoIII1 than those measured in our assay.

3.3. DrEndoIII2's preference for guanine as the opposite base

DrEndoIII2 appears to be a highly efficient bacterial EndoIII. To investigate the effect of the opposite base on the processing of the oxidized base, we performed time course assays under multiple-turnover (MTO) conditions using a DNA substrate in which Tg was paired to either adenine or guanine (Fig. 3 and Table S2). These data demonstrate that drEndoIII2 exhibits the same opposite base preference as hNTH and ecEndoIII, in that all three process Tg more efficiently when paired with guanine than with adenine. As drEndoIII2 is highly efficient, we used a low enzyme concentration of 3 nM for these assays with 75 nM of substrate. Interestingly, under these MTO conditions, no product could be detected for ecEndoIII on the adenine-paired substrate, even though its activity towards Tg:G in these conditions was relatively high (30% lower than that of drEndoIII2; Table S2). This is in agreement with our molecular beacon data (Table 2), which revealed that drEndoIII2 processes Tg:A substrate more efficiently than ecEndoIII (higher turnover rate). Compared with the human homologue, drEndoIII2 displayed an approximately four-fold faster initial bifunctional activity rate on both Tg:G and Tg:A substrates. Our molecular beacon assay had also identified drEndoIII2 as the most efficient enzyme on Tg:A, but these progress curves additionally reveal that there is an uncoupling of the enzymatic activities of hNTH on Tg paired with adenine, which is not seen for drEndoIII2. This uncoupling of hNTH's activity has been previously reported [24]. The initial rate of hNTH's glycosylase activity towards Tg:A is higher than its bifunctional activity and close to half of drEndoIII2's glycosylase activity (Table S2).

3.4. DNA binding specificity

To further investigate substrate recognition by the drEndoIII enzymes and the effect of the opposite base, we performed DNA binding studies using electrophoretic mobility shift assays (EMSA) and fluorescence polarization measurements to quantify the binding affinities towards either intact DNA or DNA containing an inert Ap site analogue, THF, that mimics the natural Ap site formed after the glycosylase reaction [60]. The Ap site analogue was introduced into a FAM-labeled 16 nt duplex DNA and was paired with either adenine or guanine (Table S1). Affinity for this substrate would provide insight into the interaction

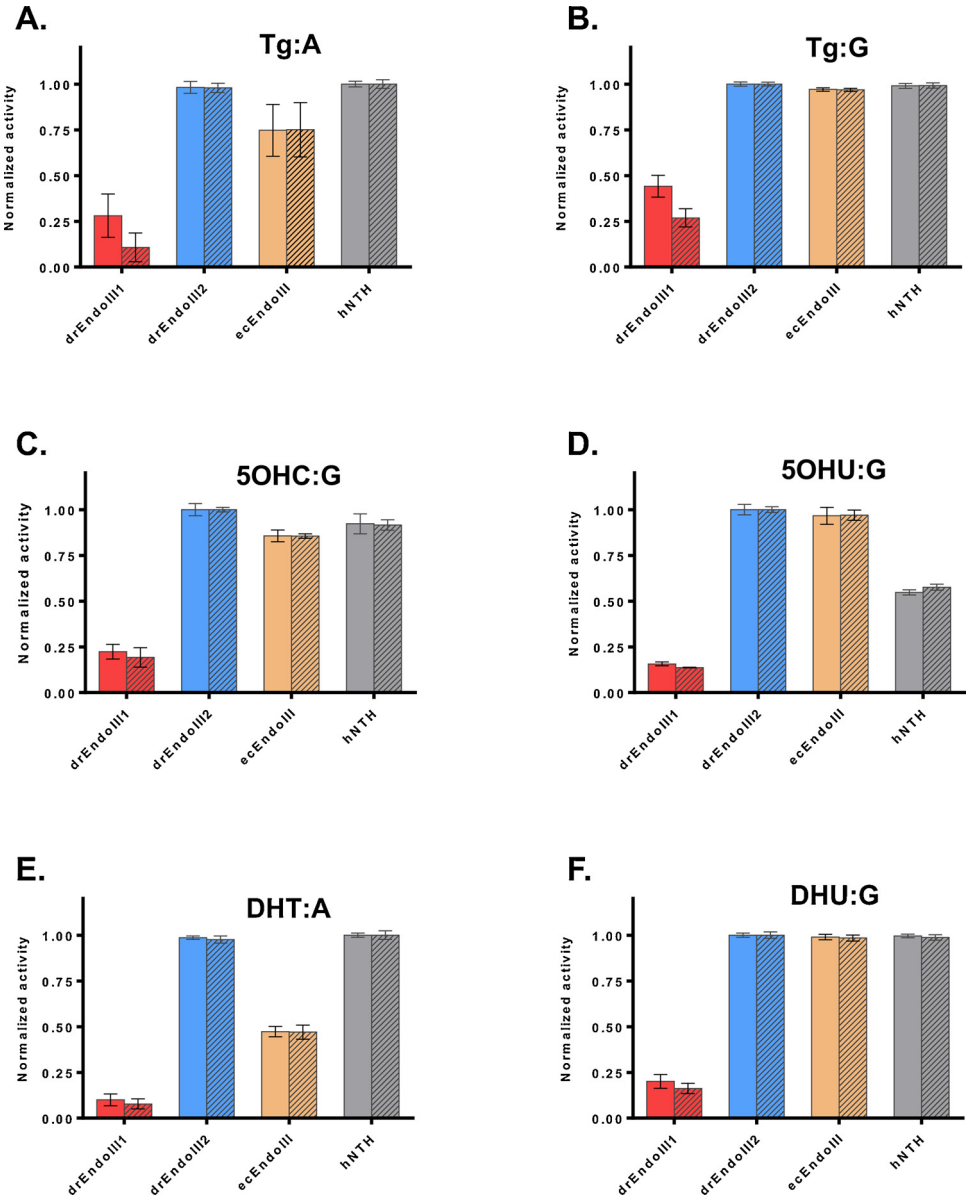

Fig. 2. Processing of oxidized bases by drEndoIII1 (red), drEndoIII2 (blue), ecEndoIII (orange) and hNTH (grey). Reactions contained 1 μM enzyme and 1 μM DNA substrate: (A) Tg:A, (B) Tg:G, (C) 5OHC:G, (D) 5OHU:G, (E) DHT:A and (F) DHU:G and were stopped after 30 min. The DNA glycosylase (plain bars) and bifunctional (striped bars) activities of drEndoIII2, which were identical under these experimental conditions, were set to 1 and the graphs thus present the relative activities of the four EndoIII enzymes. Histograms represent means and standard deviations of at least three independent experiments.

of the enzymes with the opposite base independently of the strength of the base pairing interaction. Intact, control DNA was identical except for the THF being replaced with the intact nucleoside (Table S1). Measurements were made on all three drEndoIII enzymes, as well as on hNTH for comparison and the derived dissociation constants, K_d, are presented in Table 3 and Fig. S5.

Strikingly, the affinities of all three drEndoIII enzymes towards this Ap site analogue are drastically lower than that of the human homologue and other enzymes studied previously [61–64]. The affinities of the drEndoIII enzymes for THF-containing DNA range between 30 and 660 nM, while hNTH binds with a K_d of less than 5 nM. However, both drEndoIII2 and drEndoIII3 do exhibit a clear binding specificity for the Ap site analogue compared to undamaged DNA. drEndoIII2 shows up to a 10-fold preference for THF-DNA compared to intact DNA and drEndoIII3 displays a clear preference for THF paired with guanine, with a K_d for this substrate that is at least 500 times lower than that obtained with intact DNA. Interestingly, drEndoIII3 showed a similar preference for guanine as the opposite base in EMSA binding assays with Tg or Ap site containing DNA substrates (Fig. S6). This suggests that drEndoIII3, despite being inactive on classical EndoIII substrates, can discriminate between intact and lesion containing DNA and is selective for a specific opposite base. This preference for guanine in the opposite position is also observed for drEndoIII2 (Table 3 and Fig. S6), and is in agreement with our activity measurements, which had revealed that drEndoIII2 processes guanine-paired Tg more efficiently than adenine-paired Tg. MD simulations also confirm that drEndoIII2 and drEndoIII3 both engage in conserved interactions with the estranged base via a conserved glutamine residue (Q53 in drEndoIII2 and Q61 in drEndoIII3; Fig. S7). Together these findings suggest that the more efficient excision of Tg paired with guanine is largely due to a more optimal interaction with the opposite base, and not due to slower product dissociation from the adenine-containing product.

DrEndoIII1, in contrast with the other EndoIII enzymes, displayed no selective binding to the THF containing DNA. The estimated K_d

Table 2
Catalytic parameters derived from our molecular beacon assay of thymine glycol and 5-hydroxycytosine processing by drEndoIII1, drEndoIII2, ecEndoIII and hNTH.

K_{cat} (s^{-1}) × 10^{-3}		
Protein	Thymine glycol	5-hydroxycytosine
drEndoIII1	2.77 ± 0.37	*ND*
drEndoIII2	157.50 ± 13.50	292.80 ± 32.43
ecEndoIII	41.85 ± 3.10	215.50 ± 13.35
hNTH	1.74 ± 0.05	8.29 ± 0.42
K_M (μM)		
Protein	Thymine glycol	5-hydroxycytosine
drEndoIII1	2.30 ± 0.49	*ND*
drEndoIII2	0.57 ± 0.11	0.97 ± 0.16
ecEndoIII	0.49 ± 0.05	1.44 ± 0.12
hNTH	0.04 ± 0.01	0.25 ± 0.02
K_{cat}/K_M (M^{-1} s^{-1}) × 10^3		
Protein	Thymine glycol	5-hydroxycytosine
drEndoIII1	1.20 ± 0.30	*ND*
drEndoIII2	276.32 ± 58.35	301.86 ± 59.97
ecEndoIII	85.41 ± 10.77	149.65 ± 15.54
hNTH	43.50 ± 3.49	33.16 ± 3.14

values for both undamaged and abasic DNA are very similar, in the 300 to 500 nM range. The K_d values of the other enzymes towards undamaged DNA were typically higher, in the micromolar range. DrEndoIII1 thus binds intact DNA more tightly than its homologues and is unable to discriminate between intact and abasic site containing DNA, suggesting once again that its mode of DNA binding may be different. Our failed attempts to build reliable drEndoIII1-DNA models for MD simulations (see Methods) confirmed that indeed drEndoIII1 differs greatly from its homologues in terms of DNA binding. In the DNA binding assays, the THF lesion used is not identical to the natural abasic site formed during the glycosylase reaction, since it lacks the C1' hydroxyl, which makes it resistant to cleavage by bifunctional glycosylases. As a result, its recognition by repair enzymes can be impaired. To verify this, we also performed EMSA assays to compare the binding of drEndoIII1 to DNA containing Tg, THF or the natural Ap site (produced by uracil DNA glycosylase). These assays (Fig. S6), unlike our polarization data (Table 3), reveal that drEndoIII1 does actually exhibit a preferential binding to Tg and the natural Ap site compared to THF-containing DNA. These EMSA assays also confirm our earlier observation (Table 1) that drEndoIII1 clearly discriminates against adenine in the opposite base position.

3.5. Uncoupling of drEndoIII1's enzymatic activities

The substrate screening performed at equimolar concentrations (Fig. 2) revealed an uncoupling of the two enzymatic activities of drEndoIII1, similar to that of hNTH processing of Tg:A (Fig. 3C). This effect was not observed in the initial substrate screen performed under STO conditions (Table 1). To investigate to what degree uncoupling of drEndoIII1's enzymatic activities is dependent on the enzyme concentration, we produced progress curves at varying enzyme concentrations (3, 15, 75 and 750 nM) and constant substrate concentration (75 nM). Since drEndoIII1 displays the strongest activity towards Tg paired with guanine, characterization of the uncoupling phenomenon was performed using this substrate. The full progress curves representing the DNA glycosylase activity alone and the bifunctional DNA glycosylase and AP-lyase activities, respectively, are presented in Fig. 4.

The four reaction conditions produced progress curves with distinct profiles, displaying varying degrees of bifunctional and monofunctional processing. In the condition with the least enzyme (3 nM), only glycosylase activity could be detected, while in the condition with the most enzyme (750 nM) complete bifunctional processing of the substrate was observed. The assays also reveal that both enzymatic activities of drEndoIII1 are affected by the enzyme concentration. The AP-lyase activity increases with enzyme concentration, but more intriguingly, the glycosylase activity was most efficient at the lowest enzyme concentration. Under both of the MTO conditions (Fig. 4A and B), the glycosylase reaction curves show fast initial growth, followed by rapid convergence to plateaus. The condition with 15 nM enzyme reaches a plateau at ~30% processing and the 3 nM condition at ~50% processing. Thus, the reaction with more enzyme appears to be more severely inhibited. Data analysis reveals that the initial glycosylase turnover rate under these conditions is inversely proportional to the enzyme concentration. The turnover of the 3 nM reaction is estimated to be 4-fold that of the 15 nM reaction and 9 times that of the 75 nM reaction. This observation becomes clear in the Selwyn plot presented in Fig. 4E. Such a plot reveals that drEndoIII1 is most efficient in the reaction condition with the least enzyme and strongly indicates that drEndoIII1 processing of Tg:G is not a steady state system. In the case of uncoupling, the dissociation of abasic DNA from the enzyme leads to a reaction mixture with free abasic site containing DNA, competing with the Tg substrate for enzyme binding (Fig. 1). In such a situation, the capacity of the enzyme is therefore divided between performing either the DNA glycosylase reaction or the AP-lyase reaction, and the relative engagement of the pathways depends on the concentrations of all species in the reaction mixture. Since no premature arrests were seen under STO and equimolar conditions (Fig. 4C and D), this suggests that strong product binding is most likely causing inhibition of the MTO reactions. Product inhibition has been reported previously for several DNA glycosylases, and the high affinity towards the toxic abasic site product is a critical feature of these enzymes and a means to protect the cell [25,26,28,65,66]. It is therefore not surprising that drEndoIII1 displays such a property. However, in the case of drEndoIII1, the inhibition occurs abruptly after several turnovers at a steady state rate (Fig. 4A and B). The inhibitor is therefore not likely to be the products of the glycosylase reaction (i.e. the abasic site or the free nucleobase) as is observed for other DNA glycosylases [65,67–71]. This is also supported by our binding assays (Table 3), which demonstrate that drEndoIII1 binds poorly to abasic site containing DNA. The product of the

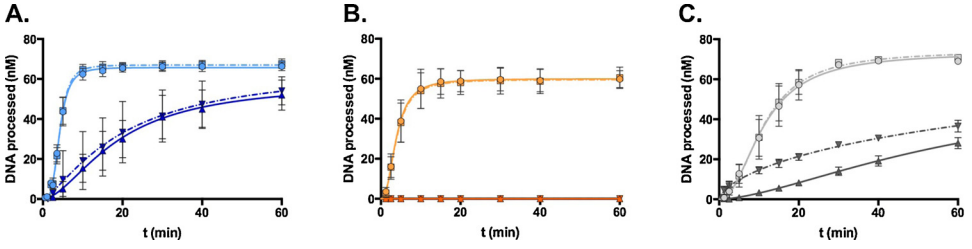

Fig. 3. Time course experiments of Tg-DNA processing by (A) drEndoIII2 (blue), (B) ecEndoIII (orange) and (C) hNTH (grey). Reactions contained 3 nM enzyme and 75 nM DNA substrate: Tg paired with adenine (dark lines) and Tg paired with guanine (pale lines). For each experiment, both the DNA glycosylase (dashed line) and the bifunctional activities (full line) were measured. Plotted values represent means and standard deviations of at least three independent experiments. Initial velocities derived from these progress curves are presented in Table S2.

Table 3
DNA binding constants (Kd) derived from fluorescence polarization measurements of drEndoIII and hNTH binding to 5'-FAM-labeled 16 nt DNA containing either an intact base or a THF in central position paired with either adenine or guanine.

Kd (nM)	drEndoIII1	drEndoIII2	drEndoIII3	hNTH
Intact T:A	313.6 ± 27.2	997.3 ± 57.5	20401 ± 7500	2430 ± 144
Intact C:G	481.4 ± 80.7	1568 ± 167	15780 ± 4980	3112 ± 198
THF:A	548.0 ± 83.7	662.4 ± 163.1	332.8 ± 15.8	4.1 ± 0.3
THF:G	417.1 ± 51.3	112.7 ± 13.0	27.6 ± 1.2	1.3 ± 0.1

AP-lyase reaction acting as the inhibitor, however, could explain our data, and indeed, binding of drEndoIII1 to nicked abasic AP-lyase product was confirmed by EMSA (Fig. S8). The onset of inhibition coincides with the appearance of the final nicked product, which could explain why the MTO reactions with more enzyme are more severely inhibited.

Our assays thus indicate that the starting enzyme concentration dictates which of the two reaction sub-pathways will be favored. Since the AP-lyase reaction would be a second order reaction dependent on both the concentrations of abasic site DNA and enzyme, an increased enzyme concentration from start would lead to an earlier engagement of this sub-pathway. This would in turn lead to accumulation of AP-lyase product and therefore an earlier enzyme inhibition, as observed in our 15 nM reaction (Fig. 4B). Other factors may also be at play, such as inhibition by the free nucleobase or dimerization of the enzyme. Interestingly, our EMSA binding assays, suggest that drEndoIII1, unlike drEndoIII2 and drEndoIII3, tends to dimerize at higher enzyme concentrations upon binding to THF-containing substrates (Fig. S8). The increased AP-lyase turnover of hNTH observed at higher enzyme concentration has been proposed to be regulated by the dimerization state of the enzyme [24]. If the AP-lyase activity of drEndoIII1 is indeed dependent on dimerization, this could also explain the observed lag in AP-lyase activity seen in our 15 and 75 nM reactions (Fig. 4B and C), which could correspond to the delay required for dimerization to take place.

3.6. ssDNA activity

UNG and Neil3 (homologue of bacterial EndoVIII), both of which are members of expanded DNA glycosylase families, have been shown to have evolved to also remove modified bases from ssDNA [29,72,73]. We therefore wondered whether one of the three EndoIII variants from *D. radiodurans* may also have specialized to process ssDNA substrates, especially as no homologues of EndoVIII have so far been identified in the *D. radiodurans* genome. Moreover, our observations that drEndoIII1 exhibits only weak activity on dsDNA substrates and appears to bind DNA in a different way, suggested that it may be a good candidate for such an activity. We thus assessed the putative activities of drEndoIII enzymes on ssDNA containing the various oxidative lesions that were tested previously in dsDNA oligonucleotides: Tg, 5OHC, 5OHU, DHT and DHU. The assay was performed with equal amounts of enzyme and substrate and both glycosylase and AP-lyase activities were assessed.

The results show that drEndoIII1 and to a lesser extent drEndoIII2, but not drEndoIII3, possess glycosylase and AP lyase activity on ssDNA substrates (Fig. 5). DrEndoIII1 excises Tg, DHU and DHT, and has weak activity on 5OHU and 5OHC substrates, which suggests it may exhibit a preference for ring-saturated substrates. As for dsDNA substrates, we observe a clear uncoupling of the glycosylase and AP lyase activities of drEndoIII1, confirming that drEndoIII1 is mostly a monofunctional enzyme capable of processing both dsDNA and ssDNA substrates. DrEndoIII2 is also able to excise oxidized pyrimidines from ssDNA with fully coupled glycosylase and AP-lyase activities, but in contrast to its high activity on dsDNA substrates (Fig. 2), this additional activity is much weaker with only 40% of the DNA being processed at best under these conditions. Its substrate specificity is also quite different from that of drEndoIII1: for both enzymes Tg is processed quite efficiently, but DHU and DHT, which are good substrates for drEndoIII1, are only poorly processed by drEndoIII2. Thus drEndoIII1 appears to possess more robust activity and broader substrate specificity than drEndoIII2 on ssDNA.

3.7. Mutational and MD studies of drEndoIIIs

We have previously established the importance of the canonical lysine and aspartate residues for Tg processing by drEndoIII1 and drEndoIII2 [13]. Mutants with either of the catalytic residues replaced by alanine (drEndoIII1 K148A and D166A, drEndoIII2 K132A and D150A) were incapable of forming a trapped Schiff base complex, as previously described for this functional class of enzymes [14]. Since the observed uncoupling of the DNA glycosylase and AP-lyase activities of drEndoIII1 and its distinct DNA binding mode indicate that drEndoIII1 and drEndoIII2 may utilize discrete catalytic mechanisms to process oxidized pyrimidines, these mutants were further tested on substrates containing either Tg or an Ap site paired with guanine generated by treatment of a uracil containing substrate with UNG. For this, equimolar enzyme:DNA reactions were performed and for the Tg-containing substrate, both the DNA glycosylase and the bifunctional activities were evaluated (Fig. 6).

Our results do indeed suggest that drEndoIII1 and drEndoIII2 may use different reaction mechanisms to process damaged DNA (Fig. 6). For both enzymes, mutations of either of the canonical catalytic residues, aspartate or lysine, completely abolished the DNA glycosylase and consequently the bifunctional activities towards the Tg substrate, in agreement with the observations from our earlier trapping assays [13].

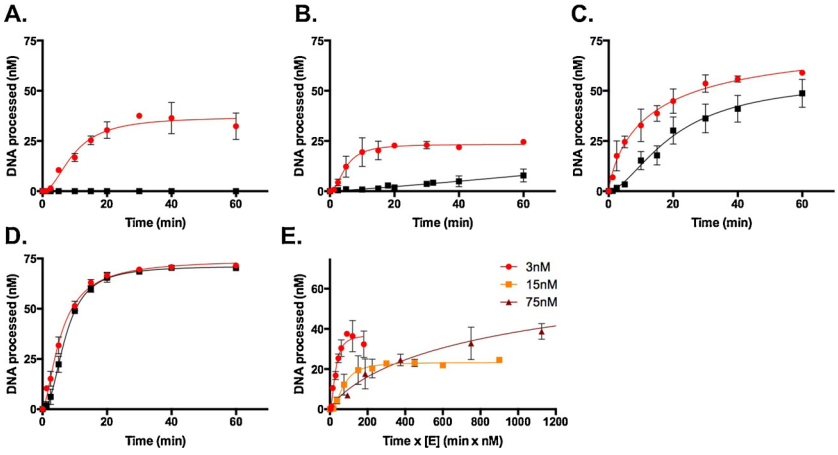

Fig. 4. Time course experiments of Tg-DNA processing by drEndoIII1. Reactions contained 75 nM Tg:G DNA and increasing amounts of drEndoIII1: (A) 3 nM, (B) 15 nM, (C) 75 nM and (D) 750 nM enzyme. For each experiment, both the DNA glycosylase (red line) and the bifunctional activities (black line) were measured. (E) Selwyn plot comparing the DNA glycosylase activity of drEndoIII1 in the reactions containing 3 nM (red), 15 nM (orange) and 75 nM (dark red) enzyme. Plotted values represent means and standard deviations of at least three independent experiments.

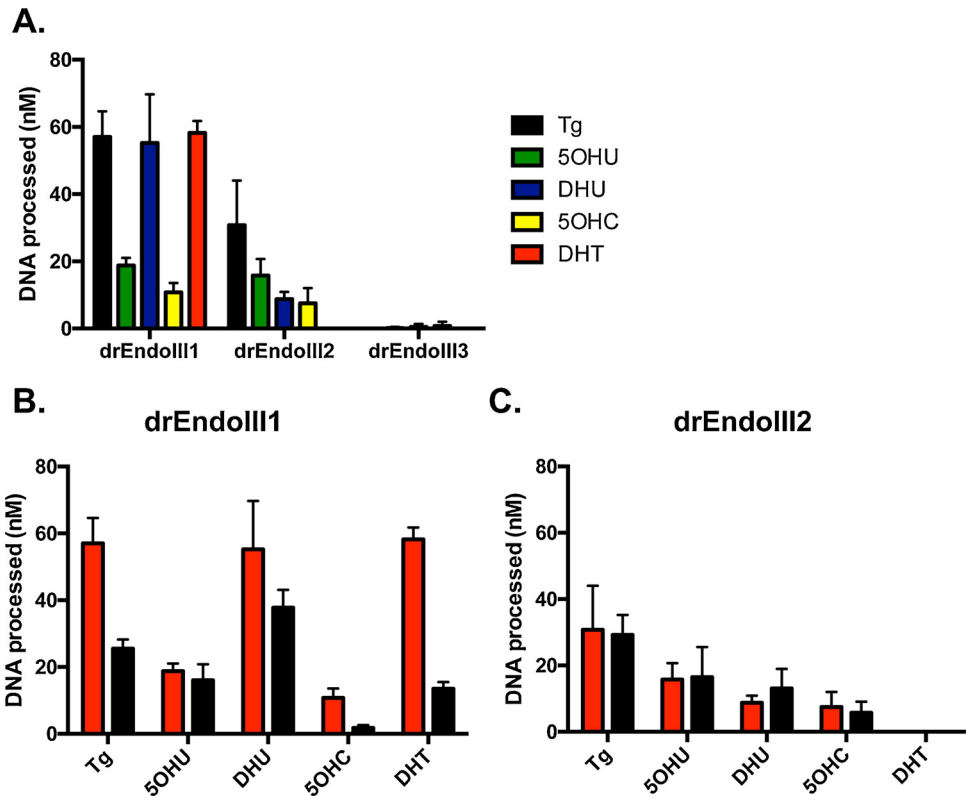

Fig. 5. ssDNA repair activities of drEndoIII enzymes. (A) DNA glycosylase activity of drEndoIII1, drEndoIII2 and drEndoIII3 on Tg (black), 5OHU (green), DHU (blue), 5OHC (yellow) or DHT (red)-containing ssDNA substrates. (B)-(C) The glycosylase (red) and bifunctional (black) activities of drEndoIII1 (B) and drEndoIII2 (C) on ssDNA substrates. The activities were assessed by gel electrophoresis after 30 min incubation of equimolar concentrations of DNA and enzyme (75 nM). Plotted values represent means and standard deviations of at least three independent experiments.

To our surprise, however, there was a notable difference between the two enzymes regarding their AP-lyase activities. For drEndoIII2, the D150A mutant displayed fully functional AP-lyase activity, while the corresponding mutation in drEndoIII1, D166A, significantly reduces the activity towards the Ap site substrate. In addition, the drEndoIII2 K132A mutant, unlike its drEndoIII1 counterpart (K148A) seems also to have retained weak AP-lyase activity. This suggests that D150, and perhaps also to a lesser extent K132, are dispensable for the AP-lyase reaction catalyzed by drEndoIII2, while the corresponding residues in drEndoIII1, in contrast, are needed for both the glycosylase and the AP-lyase reactions. The weak AP-lyase activity detected for the drEndoIII1 D166A mutant suggests that the aspartate may be more critical for the glycosylase step than for the AP-lyase step. Our MD simulations of drEndoIII2 on Tg and Ap site containing DNA substrates support these experimental findings and reveal that the catalytic aspartate is much more dynamic than the catalytic lysine (Fig. S9). With the Tg DNA and regardless of the opposite base, the two catalytic residues remain close to the damaged base and engage in stable interactions with Tg throughout the MD simulations, while with Ap DNA, these two residues adopt a wider distribution of positions during the course of the MD run (Fig. S9 and S10).

A third active site residue was mutated in the drEndoIII enzymes, based on a study by Watanabe et al that indicated that D44 of ecEndoIII may be important for the beta-elimination step of the reaction, but not

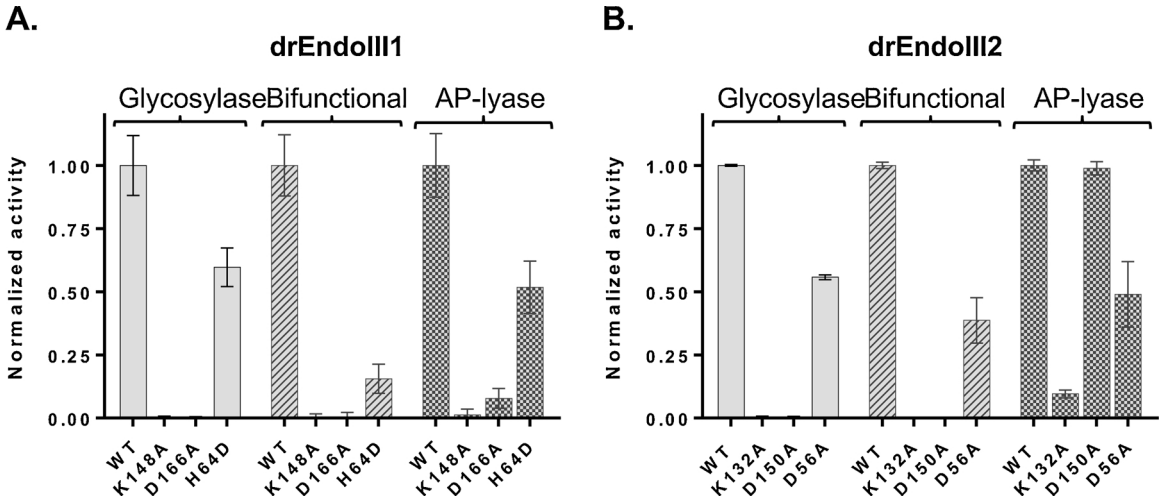

Fig. 6. Mutational study of drEndoIII1 (A) and drEndoIII2 (B) activities on Tg- and Ap site DNA. The glycosylase and bifunctional activities of wild-type (WT) and mutant enzymes were assessed using Tg:A DNA, while the AP-lyase activities were measured on Ap site containing DNA. In all reactions, equimolar concentrations of DNA and enzyme (75 nM) were incubated for 60 min and the activities of the mutants were compared to those of the WT for each enzyme-substrate condition. The WT activity was set to 1 in each case. Plotted values represent means and standard deviations of at least three independent experiments.

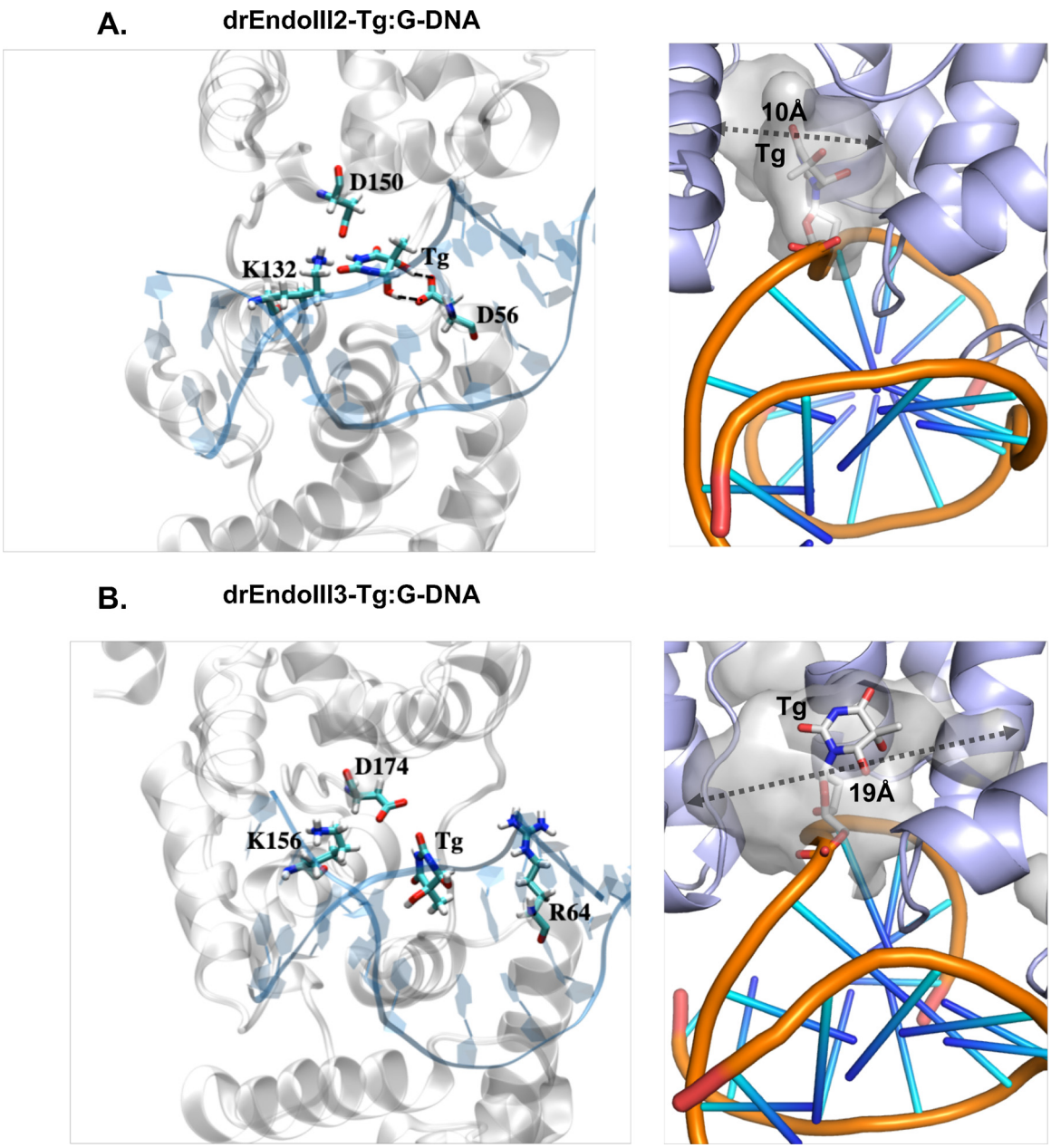

Fig. 7. Close-up view of a representative snapshot of the substrate binding pockets of drEndoIII2 (A) and drEndoIII3 (B) interacting with DNA carrying Tg paired with guanine as the estranged nucleotide. The snapshots were selected from stable regions of the MD simulations (Fig. S10). Left: The protein (grey) and DNA (blue) backbones are represented in ribbons with the two conserved catalytic residues (Asp and Lys) represented in sticks. The additional Asp residue (D56 in drEndoIII2) and its equivalent residue in drEndoIII3 (R64) are also shown in sticks. The ribose moiety of the Tg lesion is not represented for clarity. Dotted lines represent the long-lived hydrogen bonds between the hydroxyl groups of Tg and D56, which are observed throughout all MD trajectories. Right: The cavity forming the substrate binding pocket is highlighted in grey with the protein and DNA backbones coloured respectively in blue and orange. The Tg is depicted in sticks. The longest dimension of the binding pocket is indicated with a double arrow. In drEndoIII3, the Tg base is located at the periphery of the binding pocket, which is solvent accessible. In contrast, in drEndoIII2, the Tg moiety enters deep into the substrate binding pocket engaging in multiple interactions with the surrounding residues.

for the glycosylase activity [74]. This aspartate is highly conserved across EndoIII enzymes, but is not conserved in drEndoIII1 and drEndoIII3. Instead these enzymes have, respectively, a histidine and arginine, in the corresponding position (Table S3). Back-to-function mutations were therefore prepared by mutating H64 of drEndoIII1 and R64 of drEndoIII3 to aspartates to investigate whether these residues could be the cause of the weak AP-lyase activity of drEndoIII1 and the missing AP-lyase activity of drEndoIII3. The conserved aspartate in the corresponding position in drEndoIII2, D56, was also mutated to alanine to study its possible involvement in the catalytic process. The activity of these mutants was again tested on both the Tg and Ap containing DNA substrates (Fig. 6). The back-to-function mutation had no effect in drEndoIII3, and in drEndoIII1, the activities of the H64D mutant were actually reduced towards both Tg and Ap-DNA substrates, indicating that both the glycosylase and the AP-lyase reactions were affected by this mutation. H64 thus appears to be an important residue for drEndoIII1's catalytic activity. The reduction of drEndoIII1-H64D's glycosylase activity towards Tg DNA is comparable to the reduction of its AP-lyase activity towards the abasic site DNA, at about 45%. The bifunctional activity towards Tg appears to have been more severely affected, as this activity shows an 85% reduction for the H64D mutant. This may result from the uncoupling of its glycosylase and lyase activities and its

weak lyase activity at low enzyme concentration.

In the case of drEndoIII2, mutating D56 to alanine also reduced its activity towards both Tg and Ap site DNA. As with the drEndoIII1 mutant, both the AP-lyase and glycosylase activities were reduced in drEndoIII2 D56A. Although this aspartate has been shown to be dispensable for the DNA glycosylase activity of ecEndoIII [74], the equivalent mutation mostly affects the DNA glycosylase activity of hNTH [75]. Interestingly, our MD simulations of drEndoIII2 with Tg-DNA indicate that D56 may be directly involved in the recognition and stabilization of the oxidized base in the substrate binding pocket, since it is seen to form stable hydrogen-bonds with the two OH groups in Tg that differentiate it from thymine (Fig. 7). With Ap-DNA, D56 no longer interacts with the substrate, but remains nonetheless close to the abasic site throughout the simulation, which supports its possible involvement in the AP-lyase activity as well (Fig. S11). Under conditions where wild-type ecEndoIII processed Ap site substrate, Watanabe et al. observed that the ecEndoIII D44V mutant was also found to form a tight enzyme-DNA complex, which could be seen as a slow migrating band during gel electrophoresis [74]. A similar complex was observed for drEndoIII2 D56A in our assays (Fig. S12). The persistence of this complex in the denaturing gels indicates that the complex may be covalently bound, but vulnerable to the NaOH and heat treatment used to assess DNA glycosylase activity. In the absence of efficient beta-elimination, the covalently linked Schiff base complex could possibly persist for a longer period. Such a slow migrating band was never observed with drEndoIII1 samples, which suggests either that it does not form a Schiff base intermediate in performing its glycosylase activity or that the covalent Schiff base bond is efficiently hydrolyzed before beta-elimination takes place.

With the drEndoIII2-D56A and D150A mutants, we also noticed the appearance of an additional faster migrating band (Fig. S12), which most likely corresponds to the product of a delta-elimination reaction. Such a band is occasionally seen in our gels using wild-type drEndoIII2, but represents only a minor fraction of the products of the reaction. The increased fraction of delta-elimination product for the drEndoIII2 aspartate mutants is interesting and may result from inefficient hydrolysis of the Schiff base complex, allowing for delta-elimination to take place. This would be in agreement with the catalytic reaction mechanisms proposed by Dodson et al. [76].

Finally, in order to gain insight into the lack of catalytic activity of drEndoIII3 on oxidized bases, we performed MD simulations of drEndoIII3 on Tg- and Ap-DNA and examined the positions and dynamics of the conserved catalytic residues and the architecture of the substrate binding pocket. These simulations clearly showed that the catalytic residues (Lys and Asp) are highly dynamic and never engage in stable interactions with Tg in the binding pocket (Fig. 7 and Fig. S9–S11). This most likely results from the configuration of the binding pocket which differs remarkably in terms of shape, size and nature of residues lining the pocket, from that of drEndoIII2 (Fig. 7). In drEndoIII3, the Tg moiety remains at the periphery of the substrate binding pocket and never comes close to the putative catalytic residues.

4. Discussion

We had previously demonstrated that both drEndoIII1 and drEndoIII2 possess activity towards the archetypal EndoIII substrates Tg and Ap sites, while drEndoIII3 shows no activity towards these substrates [13]. In this study, we now show that drEndoIII2 has a very broad substrate specificity towards damaged pyrimidines and displays a highly efficient bifunctional activity, which relies on a high turnover rate and moderate affinity for the substrate, that is similar to, and even surpassing, that of its well-studied bacterial and human homologues: ecEndoIII and hNTH.

In contrast, drEndoIII1 appears to be an unusual EndoIII enzyme, with modified DNA binding properties. It differs greatly from drEndoIII2 in terms of catalytic activity and substrate specificity. Most noteworthy are drEndoIII1's preference for ssDNA substrates and the uncoupling of its two enzymatic activities. Uncoupling of the glycosylase and lyase activities has only previously been reported for eukaryotic DNA glycosylases: human NTH, the structurally related human Ogg1 [65,77] and the structurally non-related human Neil3 [29]. All three of these enzymes repair ROS induced base damage. The uncoupling of the two catalytic activities of DNA-glycosylases has been proposed to represent a biologically significant point of activity regulation, which can be modulated by interaction partners [25,65]. It is therefore interesting to see that this mechanism might also be applicable in bacterial DNA repair. Studies of mammalian NTH or Ogg1 suggest that these enzymes primarily perform as monofunctional DNA-glycosylases when the downstream AP-endonuclease enzyme is present [25,78] and, interestingly, human Neil3 has also been shown to process oxidized bases in ssDNA and here again mostly as a monofunctional enzyme [29]. As in eukaryotes, drEndoIII1 may thus play a complementary role to that of the robust drEndoIII2 enzyme and may function mostly as a monofunctional DNA glycosylase responsible for removal of oxidized bases in ssDNA in *D. radiodurans*.

Our mutational assays on drEndoIII1 and 2, supported by our MD simulations on drEndoIII2, reveal that the two well-established catalytic residues, K148 and D166 in drEndoIII1 and K132 and D150 in drEndoIII2, are needed for activity towards Tg and are absolutely essential for the initial DNA glycosylase activity. Regarding the AP-lyase activity, only the catalytic lysine appears to be playing a critical role. This is in agreement with the study by Dalhus et al. [79] in which they propose that the catalytic aspartate of the structurally related hOgg1 is primarily responsible for base removal during the DNA glycosylase step, while the catalytic lysine is critical for both substrate recognition during base hydrolysis and for the nucleophilic attack during the AP-lyase reaction. Mutating the aspartate residue to alanine had a contrasted effect on the AP-lyase activity of drEndoIII1 compared to drEndoIII2. In the first case, the mutation caused a severe reduction in the AP-lyase activity, while in drEndoIII2 the equivalent mutation did not seem to affect the AP-lyase activity on abasic site substrate. The exact role of this aspartate residue in the catalysis of the bifunctional reaction is unclear. Crystal structures have shown that it is structurally important as a helix capper and has been proposed to stabilize the positive charge that develops on O4' during the dissociation of the nucleobase [13,14,22]. In our various MD simulations of drEndoIII2-DNA complexes, the catalytic aspartate appears to be more dynamic than the catalytic lysine residue. Our mutational studies indicate that the involvement of the catalytic aspartate in the AP-lyase step may not be conserved throughout all EndoIII enzymes and may depend on the local architecture and orientation of the different residues composing the catalytic binding pockets of each enzyme. In drEndoIII2, structural rearrangements in the active site may compensate for the lack of D150 in the D150A mutant. The role of the aspartate in Ap site processing has also been addressed in another study of hOgg1. Norman et al [22] suggest that this aspartate is needed for the beta-elimination step and functions by orienting the ribose for proper interaction with the proton abstractor [22,80]. In the drEndoIII2-D150 A mutant, other DNA-binding residues located in the lesion-binding pocket may compensate for the absence of D150 and contribute to the correct placement of the ribose. The conserved aspartate located at the N-terminus of helix αC (D56 in drEndoIII2) has previously been suggested to act as the proton abstractor during β-elimination [14,74]. Unlike D150, this residue proved to be important for AP-lyase activity. This observation thus supports earlier studies, which proposed that D44 from ecEndoIII was needed for the beta-elimination step. However, in processing Tg containing substrate, the D56A mutation also affected the glycosylase activity, suggesting this residue is also important for recognition/discrimination during the initial flipping of the nucleotide. This effect has previously been observed in hNTH [75]; drEndoIII2 is thus more similar to hNTH than ecEndoIII in this respect. In our MD simulation of drEndoIII2 bound to Tg-DNA, D56 is indeed seen to engage in specific

contacts with the hydroxyl groups of Tg (Fig. 7).

Interestingly, the same was observed in drEndoIII1, when we mutated the equivalent residue at this position (H64) to aspartate, which we expected would enhance the AP-lyase activity. Instead, both the glycosylase and the AP-lyase activities of drEndoIII1 were reduced. So even though drEndoIII1 and drEndoIII2 do not have the same residue at this position (histidine vs. aspartate), its involvement in both steps of the catalytic reaction appears to be conserved and H64 could also act as the proton abstractor during the beta-elimination step. The closest homologues of drEndoIII1 in the *Deinococcus-Thermus* phylum have either a histidine or a tryptophan in this position, indicating that the aromatic nature of this residue may also be important and may contribute to stabilizing nucleobases in the early stages of base flipping or discriminating against undamaged bases.

DrEndoIII2 displays a very broad substrate specificity, with a clear preference for guanine in the position opposite the lesion. The stronger affinity for the Ap site analogue, THF, when paired with guanine, that we observed in our DNA binding assays (Table 3), indicates that the preference for guanine is due, in part at least, to a difference in the association with the damaged DNA substrate. The base pairing of Tg with guanine is known to be less stable than with adenine [81–83], but this is not the case for uracil [84], thus the guanine preference is not merely a result of lower energetic barrier for the base flipping step. The higher affinity for guanine in the position opposite the lesion is typical of EndoIII enzymes and has been explained by the stabilizing interaction formed between the guanine and a highly conserved glutamine in the DNA intercalating loop 1 [14] as evidenced by MD simulations (Fig. S7).

Tg paired with guanine results mainly from the oxidation and deamination of 5-methylcytosine. Cytosine methylation has recently been reported in *D. radiodurans* [85]. DrEndoIII2's preference for guanine in the opposite base position may also reflect its role in the excision of other oxidative stress-induced cytosine lesions paired with guanine, as demonstrated in our initial substrate screen (Table 1). As the *D. radiodurans* genome has five genes potentially encoding uracil DNA glycosylases [31,86,33,87], one can assume that the observed low-level uracil excision by drEndoIII2 is a side effect of its broad DNA-glycosylase activity and does not represent a major activity of drEndoIII2 *in vivo*.

Unlike drEndoIII2, drEndoIII1 did not exhibit a clear preference for guanine opposite the damaged bases. Instead, drEndoIII1 was able to process oxidized pyrimidines base-paired with guanine, thymine or cytosine, but showed significantly reduced activity on oxidized bases paired with adenine. Three of the tested substrates (Tg, DHT, DHU) have intact base pairing with adenine, which could suggest that drEndoIII1 may have a weaker ability to enforce structural perturbations and consequently flipping of the lesion [55]. However, 5OHU engages in a more stable interaction with guanine than with adenine [88,89], and yet is processed more efficiently by drEndoIII1 when paired with any base other than adenine. These observations imply that drEndoIII1 specifically selects against adenine. Unlike drEndoIII2, drEndoIII1 does not have the glutamine nucleotide flipper typical of EndoIII enzymes; instead, it has an arginine in the corresponding position, which is also found in the thymine mismatch glycosylases (MBD4, TDG, and MIG), which remove thymine from T:G mismatches and thus depend on discriminating against adenine in the opposite position [90–92].

DrEndoIII3 did not show any activity towards the oxidized pyrimidines or abasic sites tested in this study (Table 1) nor towards the most common oxidized base, 8-oxo-G, thus the substrate for this enzyme remains unknown. However, it was interesting to observe that drEndoIII3 is nonetheless capable of binding to an Ap site with guanine in the opposite position (THF:G). Remarkably, drEndoIII3 displayed a higher affinity for this substrate than drEndoIII2 (Table 3). The reason for the absence of AP-lyase activity towards Ap sites remains to be determined, but our MD data provide us with some clues. Earlier studies have shown that AP-lyase scission can be quite promiscuous in proximity of nucleophilic amines [93]. Our MD simulations reveal that the entire substrate binding pocket is reorganized in drEndoIII3 compared to that of previously studied EndoIII enzymes (Fig. 7). DrEndoIII3 is able to specifically bind to DNA substrates with modified bases paired to guanine in a similar manner to drEndoIII2, but its catalytic residues are highly dynamic and the stabilizing residues involved in binding to Tg in drEndoIII2 models are largely missing in drEndoIII3 (Fig. S9-S11). As a result, the oxidized base fails to fully enter the substrate binding pocket for processing by the enzyme and instead remains at the periphery of the binding pocket, close to the solvent. So although we cannot rule out that drEndoIII3 may have a yet unidentified substrate, a possible role for this enzyme could therefore be to prevent the processing of oxidized bases or Ap sites in conditions of high oxidative stress and thereby protect the cell from genotoxic single-strand breaks. Moreover, drEndoIII3 may also be involved in crosstalk between different DNA repair systems. For example, it may serve to recruit other DNA repair enzymes, such as proteins from the nucleotide excision repair pathway, which has been proposed to possibly function as a backup system for the repair of oxidized bases when the BER pathway is inactivated [94–96]. A similar role has been attributed to the inactive alkyltransferase-like protein, ATL, in the protection against DNA alkylation [97].

5. Conclusions

In *E. coli* and mammals, the repair of Tg has been shown to rely on the involvement of at least two enzymes [56]. One enzyme acts as the workhorse for Tg removal, while the second, backup enzyme, also excises Tg, but with lesser efficiency. In *D. radiodurans,* drEndoIII1 has been shown to be more abundant than drEndoIII2 and 3 (2:1:1 ratio) under normal growth conditions [95]. In view of the remarkable catalytic activity and broad substrate specificity of drEndoIII2, we propose that it nonetheless acts as the workhorse for the repair of oxidized pyrimidines in *D. radiodurans* (Fig. 8). In contrast, drEndoIII1, acting mostly as a monofunctional DNA glycosylase, may serve as a backup for the repair of oxidized pyrimidines as well as being responsible for removal of base lesions occurring in ssDNA during transcription and/or replication. A mutational study by Hua et al, revealed that the three drEndoIII enzyme variants are non-redundant, with each one of them contributing to the repair of spontaneous DNA damage in *D. radiodurans* [95]. Thus, despite its lack of activity, drEndoIII3 may play an alternative role in either DNA damage protection or damage sensing. Following exposure to ionizing radiation, drEndoIII1 has been shown to be down-regulated [98], in agreement with its putative role as a replication/transcription coupled ssDNA repair enzyme. These cellular functions are indeed arrested during the hours following irradiation of *D. radiodurans* [99]. Under these conditions, it is likely that the highly efficient bifunctional drEndoIII2, possibly with the support of drEndoIII3, protects the cells against the damaging effects of high intracellular ROS concentrations (Fig. 8).

Funding

This work has been supported by funding from the Research council of Norway, the FUGE and SYNKROTRON programme, the Fondation ARC pour la recherche sur le cancer (PJA 20151203255), Commissariat à l'énergie atomique et aux énergies alternatives (CEA) in the context of the 'Radiations ionisantes' programme, inhouse research funding from the European Synchrotron Radiation Facility (ESRF), Grenoble, France, an Intra-European Fellowship (IEF) within the Marie Curie actions in FP7 and the FCT; R&D projects: PTDC/QUI-BIQ/100007/2008, UID/CBQ/04612/2013 (MostMicro unit), PTDC/BB-BBEP/0561/2014 (FR) and post-doc fellowship SFRH/BPD/97493/2013 (EM). Funding for open access charge: Commissariat à l'énergie atomique et aux énergies alternatives, Radiobiology Program.

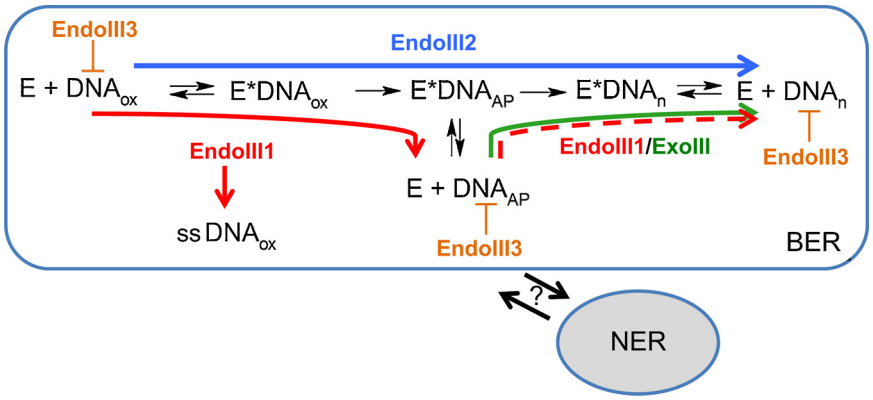

Fig. 8. Model of the respective roles and implications of drEndoIII1, drEndoIII2 and drEndoIII3 in the recognition and processing of oxidized pyrimidines in *D. radiodurans*. DrEndoIII2 represents the major EndoIII enzyme activity in cells, responsible for the efficient repair of a broad range of oxidized bases, even though drEndoIII1 has been shown to be the most abundant EndoIII enzyme in *D. radiodurans* cells under normal growth conditions. Despite its weak activity, drEndoIII1 may contribute to the repair and processing of a fraction of the oxidized bases, including damaged bases in ssDNA, but we expect this to be mainly as a monofunctional DNA glycosylase in conjunction with the AP-endonuclease enzyme (Exonuclease III or ExoIII). DrEndoIII3 may be playing an alternative role in genome maintenance, either as a protective protein or in the recruitment of additional DNA repair proteins from other pathways, such as the nucleotide excision repair (NER).

Conflict of interest

The authors declare no conflicts of interest.

Appendix A. Supplementary data

Supplementary material related to this article can be found, in the online version, at doi:https://doi.org/10.1016/j.dnarep.2019.03.014.

References

[1] B.N. Ames, M.K. Shigenaga, T.M. Hagen, Oxidants, antioxidants, and the degenerative diseases of aging, Proc. Natl. Acad. Sci. U. S. A. 90 (1993) 7915–7922 http://www.ncbi.nlm.nih.gov/entrez/query.fcgi?cmd=Retrieve&db=PubMed&dopt=Citation&list_uids=8367443.

[2] A.P. Breen, J.A. Murphy, Reactions of oxyl radicals with DNA, Free Radic. Biol. Med. 18 (1995) 1033–1077, https://doi.org/10.1016/0891-5849(94)00209-3.

[3] M. Dizdaroglu, Chemical characterization of ionizing radiation-induced damage to DNA, Biotechniques 4 (1986) 536–546.

[4] J.M. Villanueva, J. Pohl, P.W. Doetsch, L.G. Marzilli, The mutagenic damaged DNA base, 5,6-dihydrouracil (DHU), incorporated into a 14-mer duplex: NMR evidence that DHU is intrahelical and causes minimal DNA distortion [14], J. Am. Chem. Soc. (121) (1999) 10652–10653, https://doi.org/10.1021/ja9920516.

[5] J. Liu, P.W. Doetsch, *Escherichia coli* RNA and DNA polymerase bypass of dihydrouracil: mutagenic potential via transcription and replication, Nucleic Acids Res. 26 (1998) 1707–1712, https://doi.org/10.1093/nar/26.7.1707.

[6] D.I. Feig, L.C. Sowers, L.A. Loeb, Reverse chemical mutagenesis: identification of the mutagenic lesions resulting from reactive oxygen species-mediated damage to DNA, PNAS 91 (1994) 6609–6613, https://doi.org/10.1073/pnas.91.14.6609.

[7] A.A. PURMAL, G.W. LAMPMAN, Y.W. KOW, S.S. WALLACE, The sequence context-dependent mispairing of 5-hydroxycytosine and 5-hydroxyuridine in vitro, Ann. N. Y. Acad. Sci. 726 (1994) 361–363, https://doi.org/10.1111/j.1749-6632.1994.tb52852.x.

[8] A.K. Basu, E.L. Loechler, S.A. Leadon, J.M. Essigmann, Genetic effects of thymine glycol: site-specific mutagenesis and molecular modeling studies, Proc. Natl. Acad. Sci. U. S. A. 86 (1989) 7677–7681, https://doi.org/10.1073/pnas.86.20.7677.

[9] H. Ide, Y.W. Kow, S.S. Wallace, Thymine glycols and urea residues in M13 DNA constitute replicative blocks in vitro, Nucleic Acids Res. 13 (1985) 8035–8052, https://doi.org/10.1093/nar/13.22.8035.

[10] J.M. Clark, G.P. Beardsley, Thymlne glycol lesions terminate chain elongation by DNA polymerase I in vitro, Nucleic Acids Res. 14 (1986) 737–749, https://doi.org/10.1093/nar/14.2.737.

[11] M. Dizdaroglu, Base-excision repair of oxidative DNA damage by DNA glycosylases, Mutat. Res. 591 (2005) 45–59, https://doi.org/10.1016/j.mrfmmm.2005.01.033.

[12] M.M. Thayer, H. Ahern, D. Xing, R.P. Cunningham, J.A. Tainer, Novel DNA binding motifs in the DNA repair enzyme endonuclease III crystal structure, EMBO J. 14 (1995) 4108–4120 http://www.ncbi.nlm.nih.gov/entrez/query.fcgi?cmd=Retrieve&db=PubMed&dopt=Citation&list_uids=7664751.

[13] A. Sarre, M. Ökvist, T. Klar, D. Hall, A. Smalas, S. McSweeney, J. Timmins, E. Moe, Structure/function studies of two unusual Endonuclease III enzymes from the extreme radiation and desiccation resistant bacterium Deinococcus radiodurans, J. Struct. Biol. 191 (2015) 87–99.

[14] J.C. Fromme, G.L. Verdine, Structure of a trapped endonuclease III-DNA covalent intermediate, EMBO J. 22 (2003) 3461–3471 http://www.ncbi.nlm.nih.gov/entrez/query.fcgi?cmd=Retrieve&db=PubMed&dopt=Citation&list_uids=12840008.

[15] R.P. Cunningham, H. Asahara, J.F. Bank, C.P. Scholes, J.C. Salerno, K. Surerus, E. Munck, J. McCracken, J. Peisach, M.H. Emptage, Endonuclease III is an iron-sulfur protein, Biochemistry 28 (1989) 4450–4455 http://www.ncbi.nlm.nih.gov/pubmed/2548577.

[16] A.K. Boal, J.K. Barton, Electrochemical detection of lesions in DNA, Bioconjug. Chem. 16 (2005) 312–321, https://doi.org/10.1021/bc0497362.

[17] E. Moe, M. Sezer, P. Hildebrandt, S. Todorovic, Surface enhanced vibrational spectroscopic evidence for an alternative DNA-independent redox activation of endonuclease III, Chem. Commun. 51 (2015) 3255–3257, https://doi.org/10.1039/c4cc09498k.

[18] B. Demple, Enzyme structures. DNA repair flips out, Curr. Biol. 5 (1995) 719–721 http://www.ncbi.nlm.nih.gov/htbin-post/Entrez/query?db=m&form=6&dopt=r&uid=7583113.

[19] H.L. Katcher, S.S. Wallace, Characterization of the Escherichia coli X-ray endonuclease, endonuclease III, Biochemistry 22 (1983) 4071–4081 http://www.ncbi.nlm.nih.gov/pubmed/6351916.

[20] C.F. Kuo, D.E. McRee, C.L. Fisher, S.F. O'Handley, R.P. Cunningham, J. a Tainer, Atomic structure of the DNA repair [4Fe-4S] enzyme endonuclease III, Science 258 (1992) 434–440, https://doi.org/10.1126/science.1411536.

[21] J.C. Fromme, A. Banerjee, S.J. Huang, G.L. Verdine, Structural basis for removal of adenine mispaired with 8-oxoguanine by MutY adenine DNA glycosylase, Nature 427 (2004) 652–656, https://doi.org/10.1038/nature02306nature02306[pii].

[22] D.P.G. Norman, S.J. Chung, G.L. Verdine, Structural and biochemical exploration of a critical amino acid in human 8-oxoguanine glycosylase, Biochemistry 42 (2003) 1564–1572, https://doi.org/10.1021/bi026823d.

[23] D.O. Zharkov, A.A. Ishchenko, K.T. Douglas, G.A. Nevinsky, Recognition of damaged DNA by Escherichia coli Fpg protein: insights from structural and kinetic data, Mutat. Res. 531 (2003) 141–156, https://doi.org/10.1016/j.mrfmmm.2003.09.002 S0027510703001660 [pii].

[24] D.R. Marenstein, M.T.A. Ocampo, M.K. Chan, A. Altamirano, A.K. Basu, R.J. Boorstein, R.P. Cunningham, G.W. Teebor, Stimulation of human endonuclease III by Y box-binding protein 1 (DNA-binding protein B). Interaction between a base excision repair enzyme and a transcription factor, J. Biol. Chem. 276 (2001) 21242–21249, https://doi.org/10.1074/jbc.M101594200.

[25] D. Marenstein, M. Chan, A. Altamirano, A. Basu, R. Boorstein, R. Cunningham, G. Teebor, Substrate specificity of human endonuclease III (hNTH1), J. Biol. Chem. 278 (2003) 9005–9012, https://doi.org/10.1074/jbc.m212168200.

[26] M.T. Ocampo-Hafalla, A. Altamirano, A.K. Basu, M.K. Chan, J.E.A. Ocampo, A. Cummings, R.J. Boorstein, R.P. Cunningham, G.W. Teebor, Repair of thymine glycol by hNth1 and hNeil1 is modulated by base pairing and cis-trans epimerization, DNA Repair (Amst.) 5 (2006) 444–454, https://doi.org/10.1016/j.dnarep.2005.12.004.

[27] J.W. Hill, T.K. Hazra, T. Izumi, S. Mitra, Stimulation of human 8-oxoguanine-DNA glycosylase by AP-endonuclease: potential coordination of the initial steps in base excision repair, Nucleic Acids Res. 29 (2001) 430–438, https://doi.org/10.1093/nar/29.2.430.

[28] A.E. Vidal, I.D. Hickson, S. Boiteux, J.P. Radicella, Mechanism of stimulation of the DNA glycosylase activity of hOGG1 by the major human AP endonuclease: bypass of the AP lyase activity step, Nucleic Acids Res. 29 (2001) 1285–1292, https://doi.org/10.1093/nar/29.6.1285.

[29] S.Z. Krokeide, J.K. Laerdahl, M. Salah, L. Luna, F.H. Cederkvist, A.M. Fleming, C.J. Burrows, B. Dalhus, M. Bjørås, Human NEIL3 is mainly a monofunctional DNA glycosylase removing spiroimindiohydantoin and guanidinohydantoin, DNA Repair (Amst.) 12 (2013) 1159–1164, https://doi.org/10.1016/j.dnarep.2013.04.026.

[30] M.M. Cox, J.R. Battista, Deinococcus radiodurans – the consummate survivor, Nat. Rev. Microbiol. 3 (2005) 882–892, https://doi.org/10.1038/nrmicro1264.

[31] K.S. Makarova, L. Aravind, Y.I. Wolf, R.L. Tatusov, K.W. Minton, E.V. Koonin, M.J. Daly, Genome of the extremely radiation-resistant bacterium Deinococcus radiodurans viewed from the perspective of comparative genomics, Microbiol. Mol. Biol. Rev. 65 (2001) 44–79 http://www.ncbi.nlm.nih.gov/entrez/query.fcgi?cmd=Retrieve&db=PubMed&dopt=Citation&list_uids=11238985.

[32] A. Sarre, M. Okvist, T. Klar, E. Moe, J. Timmins, Expression, purification and crystallization of two endonuclease III enzymes from Deinococcus radiodurans, Acta Crystallogr. F Struct. Biol. Commun. 70 (2014) 1688–1692, https://doi.org/10.1107/S2053230X14024935S2053230X14024935[pii].

[33] H.L. Pedersen, K.A. Johnson, C.E. McVey, I. Leiros, E. Moe, Structure determination

of uracil-DNA N-glycosylase from Deinococcus radiodurans in complex with DNA, Acta Crystallogr. D Biol. Crystallogr. 71 (2015) 2137–2149, https://doi.org/10.1107/S1399004715014157S1399004715014157[pii].
[34] H. Kasai, Z. Yamaizumi, Photosensitized formation of 7,8-dihydro-8-oxo-2′-deoxyguanosine (8-hydroxy-2′-deoxyguanosine) in DNA by riboflavin: a non singlet oxygen-mediated reaction, J. Am. Chem. Soc. 114 (1992) 9692–9694, https://doi.org/10.1021/ja00050a078.
[35] J.-L. Ravanat, T. Douki, P. Duez, E. Gremaud, K. Herbert, T. Hofer, L. Lasserre, C. Saint-Pierre, A. Favier, J. Cadet, Cellular background level of 8-oxo-7,8-dihydro-2'-deoxyguanosine: an isotope based method to evaluate artefactual oxidation of DNA during its extraction and subsequent work-up, Carcinogenesis 23 (2002) 1911–1918, https://doi.org/10.1093/carcin/23.11.1911.
[36] V.J. LiCata, A.J. Wowor, Applications of fluorescence anisotropy to the study of Protein-DNA interactions, Methods Cell Biol. 84 (2008) 243–262, https://doi.org/10.1016/S0091-679X(07)84009-X.
[37] W.L. Jorgensen, J. Chandrasekhar, J.D. Madura, R.W. Impey, M.L. Klein, Comparison of simple potential functions for simulating liquid water, J. Chem. Phys. 79 (1983) 926–935, https://doi.org/10.1038/189771a0.
[38] A. Perez, I. Marchán, D. Svozil, J. Sponer, T.E. Cheatham, C.A. Laughton, M. Orozco, Refinement of the AMBER force field for nucleic acids: improving the description of alphaγconformers, Biophys. J. 92 (2007) 3817–3829, https://doi.org/10.1529/biophysj.106.097782.
[39] I. Ivani, P.D. Dans, A. Noy, A. Pérez, I. Faustino, A. Hospital, J. Walther, P. Andrio, R. Goñi, A. Balaceanu, G. Portella, F. Battistini, J.L. Gelpí, C. González, M. Vendruscolo, C.A. Laughton, S.A. Harris, D.A. Case, M. Orozco, Parmbsc1: a refined force field for DNA simulations, Nat. Methods 13 (2015) 55–58, https://doi.org/10.1038/nmeth.3658.
[40] A.T.P. Carvalho, M. Swart, Electronic structure investigation and parametrization of biologically relevant iron-sulfur clusters, J. Chem. Inf. Model. 54 (2014) 613–620, https://doi.org/10.1021/ci400718m.
[41] A.T.P. Carvalho, M. Swart, Correction for electronic structure investigation and parametrization of biologically relevant iron–sulfur clusters, J. Chem. Inf. Model. 55 (2015) 1508, https://doi.org/10.1021/acs.jcim.5b00390.
[42] E. Bignon, H. Gattuso, C. Morell, F. Dehez, A.G. Georgakilas, A. Monari, E. Dumont, Correlation of bistranded clustered abasic DNA lesion processing with structural and dynamic DNA helix distortion, Nucleic Acids Res. 44 (2016) 8588–8599, https://doi.org/10.1093/nar/gkw773.
[43] H. Gattuso, E. Durand, E. Bignon, C. Morell, A.G. Georgakilas, E. Dumont, C. Chipot, F. Dehez, A. Monari, Repair rate of clustered abasic DNA lesions by human endonuclease: molecular bases of sequence specificity, J. Phys. Chem. Lett. 7 (2016) 3760–3765, https://doi.org/10.1021/acs.jpclett.6b01692.
[44] D.A. Case, J.T. Berryman, R.M. Betz, D.S. Cerutti I.I.I., T.E. Cheatham, T.A. Darden, R.E. Duke, T.J. Giese, H. Gohlke, A.W. Goetz, N. Homeyer, S. Izadi, P. Janowski, J. Kaus, A. Kovalenko, T.S. Lee, S. Le Grand, P.L.T. Luchko, R. Luo, d K.M.M.B. Madej a, G. Monard, P. Needham, H.T. Nguyen, H.T. Nguyen, I. Omelyan, A. Onufriev, D.R. Roe, A. Roitberg, R. Salomon-Ferrer, C.L. Simmerling, W. Smith, J. Swails, R.C. Walker, J. Wang, R.M. Wolf, X. Wu, D.M. York, P.A. Kollman, T.E. Cheatham III, T.A. Darden, R.E. Duke, T.J. Giese, H. Gohlke, A.W. Goetz, N. Homeyer, S. Izadi, P. Janowski, J. Kaus, A. Kovalenko, T.S. Lee, S. LeGrand, P. Li, T. Luchko, R. Luo, B. Madej, K.M. Merz, G. Monard, P. Needham, H.T. Nguyen, H.T. Nguyen, I. Omelyan, A. Onufriev, D.R. Roe, A. Roitberg, R. Salomon-Ferrer, C.L. Simmerling, W. Smith, J. Swails, R.C. Walker, J. Wang, R.M. Wolf, X. Wu, D.M. York, P.A. Kollman, D.A.C, et al., AMBER 2015, AMBER 15, Universiyt Calif., San Fr, 2015.
[45] D.A. Case, T.E. Cheatham, T. Darden, H. Gohlke, R. Luo, K.M. Merz, A. Onufriev, C. Simmerling, B. Wang, R.J. Woods, The Amber biomolecular simulation programs, J. Comput. Chem. 26 (2005) 1668–1688, https://doi.org/10.1002/jcc.20290.
[46] W. Humphrey, A. Dalke, K. Schulten, VMD: visual molecular dynamics, J. Mol. Graph. 14 (1996) 33–38, https://doi.org/10.1016/0263-7855(96)00018-5.
[47] J.C. Phillips, R. Braun, W. Wang, J. Gumbart, E. Tajkhorshid, E. Villa, C. Chipot, R.D. Skeel, L. Kalé, K. Schulten, Scalable molecular dynamics with NAMD, J. Comput. Chem. 26 (2005) 1781–1802, https://doi.org/10.1002/jcc.20289.
[48] S.E. Feller, Y. Zhang, R.W. Pastor, B.R. Brooks, Constant pressure molecular dynamics simulation: the Langevin piston method, J. Chem. Phys. 103 (1995) 4613–4621, https://doi.org/10.1063/1.470648.
[49] G.J. Martyna, D.J. Tobias, M.L. Klein, Constant pressure molecular dynamics algorithms, J. Chem. Phys. 101 (1994) 4177–4189, https://doi.org/10.1063/1.467468.
[50] T. Darden, D. York, L. Pedersen, Particle mesh Ewald: An N·log(N) method for Ewald sums in large systems, J. Chem. Phys. 98 (1993) 10089–10092, https://doi.org/10.1063/1.464397.
[51] H.C. Andersen, Rattle: a "velocity" version of the shake algorithm for molecular dynamics calculations, J. Comput. Phys. 52 (1983) 24–34, https://doi.org/10.1016/0021-9991(83)90014-1.
[52] M. Tuckerman, B.J. Berne, G.J. Martyna, Reversible multiple time scale molecular dynamics, J. Chem. Phys. 97 (1992) 1990–2001, https://doi.org/10.1063/1.463137.
[53] S. Boiteux, F. Coste, B. Castaing, Repair of 8-oxo-7,8-dihydroguanine in prokaryotic and eukaryotic cells: properties and biological roles of the Fpg and OGG1 DNA N-glycosylases, Free Radic. Biol. Med. 107 (2017) 179–201, https://doi.org/10.1016/j.freeradbiomed.2016.11.042.
[54] T.K. Hazra, J.G. Muller, R.C. Manuel, C.J. Burrows, R.S. Lloyd, S. Mitra, Repair of hydantoins, one electron oxidation product of 8-oxoguanine, by DNA glycosylases of Escherichia coli, Nucleic Acids Res. 29 (2001) 1967–1974, https://doi.org/10.1093/nar/29.9.1967.
[55] K. Asagoshi, H. Odawara, H. Nakano, T. Miyano, H. Terato, Y. Ohyama, S. Seki, H. Ide, Comparison of substrate specificities of Escherichia coli endonuclease III and its mouse homologue (mNTH1) using defined oligonucleotide substrates, Biochemistry 39 (2000) 11389–11398, https://doi.org/10.1021/bi000422l.
[56] H. Miller, A.S. Fernandes, E. Zaika, M.M. McTigue, M.C. Torres, M. Wente, C.R. Iden, A.P. Grollman, Stereoselective excision of thymine glycol from oxidatively damaged DNA, Nucleic Acids Res. 32 (2004) 338–345, https://doi.org/10.1093/nar/gkh190.
[57] A. Katafuchi, T. Nakano, A. Masaoka, H. Terato, S. Iwai, F. Hanaoka, H. Ide, Differential specificity of human and Escherichia coli endonuclease III and VIII homologues for oxidative base lesions, J. Biol. Chem. 279 (2004) 14464–14471, https://doi.org/10.1074/jbc.M400393200.
[58] S. Senturker, C. Bauche, J. Laval, M. Dizdaroglu, Substrate specificity of Deinococcus radiodurans Fpg protein, Biochemistry 38 (1999) 9435–9439, https://doi.org/10.1021/bi990680mbi990680m[pii].
[59] X. Liu, R. Roy, Truncation of amino-terminal tail stimulates activity of human endonuclease III (hNTH1), J. Mol. Biol. 321 (2002) 265–276, https://doi.org/10.1016/S0022-2836(02)00623-X.
[60] M. Takeshita, C.N. Chang, F. Johnson, S. Will, A.P. Grollman, Oligodeoxynucleotides containing synthetic abasic sites. Model substrates for DNA polymerases and apurinic/apyrimidinic endonucleases, J. Biol. Chem. 262 (1987) 10171–10179.
[61] A.M. Chu, J.C. Fettinger, S.S. David, Profiling base excision repair glycosylases with synthesized transition state analogs, Bioorganic Med. Chem. Lett. 21 (2011) 4969–4972, https://doi.org/10.1016/j.bmcl.2011.05.085.
[62] P.A. van der Kemp, J.B. Charbonnier, M. Audebert, S. Boiteux, Catalytic and DNA-binding properties of the human Ogg1 DNA N-glycosylase/AP lyase: biochemical exploration of H270, Q315 and F319, three amino acids of the 8-oxoguanine-binding pocket, Nucleic Acids Res. 32 (2004) 570–578, https://doi.org/10.1093/nar/gkh224.
[63] O.D. Schärer, H.M. Nash, J. Jiricny, J. Laval, G.L. Verdine, Specific binding of a designed pyrrolidine abasic site analog to multiple DNA glycosylases, J. Biol. Chem. 273 (1998) 8592–8597, https://doi.org/10.1074/jbc.273.15.8592.
[64] N.A. Kuznetsov, V.V. Koval, D.O. Zharkov, O.S. Fedorova, Conformational dynamics of the interaction of Escherichia coli endonuclease VIII with DNA substrates, DNA Repair (Amst). 11 (2012) 884–891, https://doi.org/10.1016/j.dnarep.2012.08.004.
[65] I. Morland, L. Luna, E. Gustad, E. Seeberg, M. Bjørås, Product inhibition and magnesium modulate the dual reaction mode of hOgg1, DNA Repair (Amst.) 4 (2005) 381–387, https://doi.org/10.1016/j.dnarep.2004.11.002.
[66] S.L. Porello, A.E. Leyes, S.S. David, Single-turnover and pre-steady-state kinetics of the reaction of the adenine glycosylase MutY with mismatch-containing DNA substrates, Biochemistry 37 (1998) 14756–14764, https://doi.org/10.1021/bi981594+.
[67] B. Kavli, O. Sundheim, M. Akbari, M. Otterlei, H. Nilsen, F. Skorpen, P.A. Aas, L. Hagen, H.E. Krokan, G. Slupphaug, hUNG2 is the major repair enzyme for removal of uracil from U:a matches, U:g mismatches, and U in single-stranded DNA, with hSMUG1 as a broad specificity backup, J. Biol. Chem. 277 (2002) 39926–39936, https://doi.org/10.1074/jbc.M207107200.
[68] S. Grippon, Q. Zhao, T. Robinson, J.J.T. Marshall, R.J. O'Neill, H. Manning, G. Kennedy, C. Dunsby, M. Neil, S.E. Halford, P.M.W. French, G.S. Baldwin, Differential modes of DNA binding by mismatch uracil DNA glycosylase from Escherichia coli: implications for abasic lesion processing and enzyme communication in the base excision repair pathway, Nucleic Acids Res. 39 (2011) 2593–2603, https://doi.org/10.1093/nar/gkq913.
[69] U. Hardeland, R. Steinacher, J. Jiricny, P. Schär, Modification of the human thymine-DNA glycosylase by ubiquitin-like proteins facilitates enzymatic turnover, EMBO J. 21 (2002) 1456–1464, https://doi.org/10.1093/emboj/21.6.1456.
[70] S. Adhikari, A. Üren, R. Roy, Excised damaged base determines the turnover of human N-methylpurine-DNA glycosylase, DNA Repair (Amst.) 8 (2009) 1201–1206, https://doi.org/10.1016/j.dnarep.2009.06.005.
[71] T.R. Waters, P.F. Swann, Kinetics of the action of thymine DNA glycosylase, J. Biol. Chem. 273 (1998) 20007–20014, https://doi.org/10.1074/jbc.273.32.20007.
[72] G. Slupphaug, I. Eftedal, B. Kavli, S. Bharati, N.M. Helle, T. Haug, D.W. Levine, H.E. Krokan, Properties of a recombinant human uracil-DNA glycosylase from the UNG gene and evidence that UNG encodes the major uracil-DNA glycosylase, Biochemistry 34 (1995) 128–138 http://www.ncbi.nlm.nih.gov/htbin-post/Entrez/query?db=m&form=6&dopt=r&uid=7819187.
[73] I.R. Grin, D.O. Zharkov, Eukaryotic endonuclease VIII-like proteins: new components of the base excision DNA repair system, Biochem. Biokhimiia. 76 (2011) 80–93, https://doi.org/10.1134/S000629791101010X.
[74] T. Watanabe, J.O. Blaisdell, S.S. Wallace, J.P. Bond, Engineering functional changes in Escherichia coli endonuclease III based on phylogenetic and structural analyses, J. Biol. Chem. 280 (2005) 34378–34384, https://doi.org/10.1074/jbc.M504916200.
[75] S.M. Robey-Bond, M.A. Benson, R. Barrantes-Reynolds, J.P. Bond, S.S. Wallace, Probing the activity of NTHL1 orthologs by targeting conserved amino acid residues, DNA Repair (Amst.) 53 (2017) 43–51, https://doi.org/10.1016/j.dnarep.2017.02.014.
[76] M.L. Dodson, R.S. Lloyd, Mechanistic comparisons among base excision repair glycosylases, Free Radic. Biol. Med. 32 (2002) 678–682, https://doi.org/10.1016/S0891-5849(02)00767-0.
[77] M. Bjørås, L. Luna, B. Johnson, E. Hoff, T. Haug, T. Rognes, E. Seeberg, Opposite base-dependent reactions of a human base excision repair enzyme on DNA containing 7,8-dihydro-8-oxoguanine and abasic sites, EMBO J. 16 (1997) 6314–6322, https://doi.org/10.1093/emboj/16.20.6314.

[78] D.O. Zharkov, T.A. Rosenquist, S.E. Gerchman, A.P. Grollman, Substrate specificity and reaction mechanism of murine 8-oxoguanine-DNA glycosylase, J. Biol. Chem. 275 (2000) 28607–28617, https://doi.org/10.1074/jbc.M002441200.
[79] B. Dalhus, M. Forsbring, I.H. Helle, E.S. Vik, R.J. Forstrøm, P.H. Backe, I. Alseth, M. Bjørs, Separation-of-function mutants unravel the dual-reaction mode of human 8-oxoguanine DNA glycosylase, Structure 19 (2011) 117–127, https://doi.org/10.1016/j.str.2010.09.023.
[80] A. Mazumder, J.A. Gerlt, M.J. Absalon, J. Stubbe, R.P. Cunningham, J. Withka, P.H. Bolton, Stereochemical studies of the beta-elimination reactions at aldehydic abasic sites in DNA: endonuclease III from Escherichia coli, sodium hydroxide, and Lys-Trp-Lys, Biochemistry 30 (1991) 1119–1126 http://www.ncbi.nlm.nih.gov/pubmed/1846560.
[81] J.M. Clark, G.P. Beardsley, Functional effects of cis-thymine glycol lesions on DNA synthesis in vitro, Biochemistry 26 (1987) 5398–5403, https://doi.org/10.1021/bi00391a027.
[82] K.L. Brown, A.K. Basu, M.P. Stone, The cis-(5R,6S)-thymine glycol lesion occupies the wobble position when mismatched with deoxyguanosine in DNA, Biochemistry 48 (2009) 9722–9733, https://doi.org/10.1021/bi900695e.
[83] K.L. Brown, M. Roginskaya, Y. Zou, A. Altamirano, A.K. Basu, M.P. Stone, Binding of the human nucleotide excision repair proteins XPA and XPC/HR23B to the 5R-thymine glycol lesion and structure of the cis-(5R,6S) thymine glycol epimer in the 5′-GTgG-3′ sequence: Destabilization of two base pairs at the lesion site, Nucleic Acids Res. 38 (2009) 428–440, https://doi.org/10.1093/nar/gkp844.
[84] D.E. Volk, V. Thiviyanathan, A. Somasunderam, D.G. Gorenstein, Ab initio base-pairing energies of an oxidized thymine product, 5-formyluracil, with standard DNA bases at the BSSE-free DFT and MP2 theory levels, Org. Biomol. Chem. 5 (2007) 1554, https://doi.org/10.1039/b702755a.
[85] N.A. Patil, B. Basu, D.D. Deobagkar, S.K. Apte, D.N. Deobagkar, Putative DNA modification methylase DR_C0020 of Deinococcus radiodurans is an atypical SAM dependent C-5 cytosine DNA methylase, Biochim. Biophys. Acta – Gen. Subj. 1861 (2017) 593–602, https://doi.org/10.1016/j.bbagen.2016.12.025.
[86] I. Leiros, E. Moe, A.O. Smalas, S. McSweeney, Structure of the uracil-DNA N-glycosylase (UNG) from Deinococcus radiodurans, Acta Crystallogr. D Biol. Crystallogr. 61 (2005) 1049–1056 http://www.ncbi.nlm.nih.gov/entrez/query.fcgi?cmd=Retrieve&db=PubMed&dopt=Citation&list_uids=16041069.
[87] M. Sandigursky, S. Sandigursky, P. Sonati, M.J. Daly, W.A. Franklin, Multiple uracil-DNA glycosylase activities in Deinococcus radiodurans, DNA Repair 3 (2004) 163–169 http://www.ncbi.nlm.nih.gov/entrez/query.fcgi?cmd=Retrieve&db=PubMed&dopt=Citation&list_uids=14706350.
[88] V. Thiviyanathan, A. Somasunderam, D.E. Volk, T.K. Hazra, S. Mitra, D.G. Gorenstein, Base-pairing properties of the oxidized cytosine derivative, 5-hydroxy uracil, Biochem. Biophys. Res. Commun. 366 (2008) 752–757, https://doi.org/10.1016/j.bbrc.2007.12.010.
[89] V. Thiviyanathan, A. Somasunderam, D.E. Volk, D.G. Gorenstein, {5-Hydroxyuracil} can form stable base pairs with all four bases in a {DNA} duplex, Chem. Commun. (2005) 400, https://doi.org/10.1039/b414474k.
[90] J.H. Yoon, S. Iwai, T.R. O'Connor, G.P. Pfeifer, Human thymine DNA glycosylase (TDG) and methyl-CpG-binding protein 4 (MBD4) excise thymine glycol (Tg) from a Tg:G mispair, Nucleic Acids Res. 31 (2003) 5399–5404, https://doi.org/10.1093/nar/gkg730.
[91] H. Hashimoto, Structural and mutation studies of two DNA demethylation related glycosylases: MBD4 and TDG, Biophysics (Oxf.) 10 (2014) 63–68, https://doi.org/10.2142/biophysics.10.63.
[92] T.J. Begley, B.J. Haas, J.C. Morales, E.T. Kool, R.P. Cunningham, Kinetics and binding of the thymine-DNA mismatch glycosylase, Mig-Mth, with mismatch-containing DNA substrates, DNA Repair (Amst.) 2 (2003) 107–120, https://doi.org/10.1016/S1568-7864(02)00190-8.
[93] A.J. Kurtz, M.L. Dodson, R.S. Lloyd, Evidence for multiple imino intermediates and identification of reactive nucleophiles in peptide-catalyzed β-elimination at abasic sites, Biochemistry 41 (2002) 7054–7064, https://doi.org/10.1021/bi020026y.
[94] G. Dianov, C. Bischoff, J. Piotrowski, A. Vilhelm, Bohr, Repair pathways for processing of 8-oxoguanine in DNA by mammalian cell extracts, J. Biol. Chem. 273 (1998) 33811–33816, https://doi.org/10.1074/jbc.273.50.33811.
[95] X. Hua, X. Xu, M. Li, C. Wang, B. Tian, Y. Hua, Three nth homologs are all required for efficient repair of spontaneous DNA damage in Deinococcus radiodurans, Extremophiles 16 (2012) 477–484, https://doi.org/10.1007/s00792-012-0447-y.
[96] R.L. Swanson, N.J. Morey, P.W. Doetsch, S. Jinks-Robertson, Overlapping specificities of base excision repair, nucleotide excision repair, recombination, and translesion synthesis pathways for DNA base damage in Saccharomyces cerevisiae, Mol. Cell. Biol. 19 (1999) 2929–2935.
[97] J.L. Tubbs, J.A. Tainer, Alkyltransferase-like proteins: molecular switches between DNA repair pathways, Cell. Mol. Life Sci. 67 (2010) 3749–3762, https://doi.org/10.1007/s00018-010-0405-8.
[98] Y. Liu, J. Zhou, M.V. Omelchenko, A.S. Beliaev, A. Venkateswaran, J. Stair, L. Wu, D.K. Thompson, D. Xu, I.B. Rogozin, E.K. Gaidamakova, M. Zhai, K.S. Makarova, E.V. Koonin, M.J. Daly, Transcriptome dynamics of Deinococcus radiodurans recovering from ionizing radiation, Proc. Natl. Acad. Sci. U. S. A. 100 (2003) 4191–4196 http://www.ncbi.nlm.nih.gov/entrez/query.fcgi?cmd=Retrieve&db=PubMed&dopt=Citation&list_uids=12651953.
[99] D. Slade, A.B. Lindner, G. Paul, M. Radman, Recombination and replication in DNA repair of heavily irradiated Deinococcus radiodurans, Cell 136 (2009) 1044–1055, https://doi.org/10.1016/j.cell.2009.01.018.